Distance metrology using optical frequency comb a step closer to industrial applications

Hei, K.

DOI
10.4233/uuid:791a858e-c194-47bc-b57c-43346001b41b

Publication date
2021

Document Version
Final published version

Citation (APA)
Hei, K. (2021). *Distance metrology using optical frequency comb a step closer to industrial applications*. [Dissertation (TU Delft), Delft University of Technology]. https://doi.org/10.4233/uuid:791a858e-c194-47bc-b57c-43346001b41b

DISTANCE METROLOGY USING OPTICAL FREQUENCY COMB A STEP CLOSER TO INDUSTRIAL APPLICATIONS

DISTANCE METROLOGY USING OPTICAL FREQUENCY COMB A STEP CLOSER TO INDUSTRIAL APPLICATIONS

Proefschrift

ter verkrijging van de graad van doctor
aan de Technische Universiteit Delft,
op gezag van de Rector Magnificus Prof.dr.ir. T.H.J.J. van der Hagen,
voorzitter van het College voor Promoties,
in het openbaar te verdedigen op vrijdag 16 juli 2021 om 10:00 uur

door

Kefei HEI

Master of Engineering in Information and Communication Engineering,
Tianjin University, China,
geboren te Jilin, China.

Dit proefschrift is goedgekeurd door de

promotor: Dr. N. Bhattacharya
copromotor: Dr. E.C.M. Carroll

Samenstelling promotiecommissie:

Rector Magnificus,	voorzitter
Dr. N. Bhattacharya,	Technische Universiteit Delft, promotor
Dr. E.C.M. Carroll,	Technische Universiteit Delft, copromotor
Onafhankelijke leden:	
Prof. dr. U. Staufer	Technische Universiteit Delft
Prof. dr. ir. J.L. Herder	Technische Universiteit Delft
Dr. P. Anandarajah	Dublin City U. Ireland
Dr. E.A.J.M. Bente,	TU Eindhoven
Dr. S.A. van den Berg,	The Hague U. of Applied Science

Keywords: Frequency Comb, Distance Metrology, Integrated Optics

Printed by: Ipskamp Printing

Front & Back: Spectrum of a typical optical frequency comb in frequency domain and serious of pulses in time domain.

ISBN 000-00-0000-000-0

An electronic version of this dissertation is available at
http://repository.tudelft.nl/.

CONTENTS

SUMMARY

Length is one of the fundamental physical quantities and its precise measurement is very important for science and technology. Laser-based distance metrology technique is a powerful tool, which is widely applied in geodetic monitoring, environmental monitoring and precision measurement engineering including in space applications. Since the invention of the optical frequency comb (OFC) at the beginning of this century, it has been used as a versatile tool for many applications, such as frequency metrology, spectroscopy, etc. OFC has played an important role in distance metrology enabling the developed techniques to achieve high accuracy in long distance measurement. In the time domain, OFC is a pulse train, which can measure distance with time of flight method or correlation detection method. In the frequency domain, spectrum of OFC consists of a series of discrete lines with equal frequency difference. Methods of dispersive interferometry, multi-heterodyne interferometry, and multi-wavelength interferometry are the techniques proposed and demonstrated in spectral domain distance metrology. Though distance metrology techniques based on OFC have been developed for tens of years, there are still challenges that need to be overcome. In most applications the measurements are completed in the air, where the results are influenced by refractive index of air. As the OFC is a multi-wavelength laser source, refractive index of air is difficult to determine. The other challenge is complexity and high cost of measurement system. Until now, to my knowledge, there is no commercial rangefinder which is based on OFC. The large size, complex configuration and high price are the bottlenecks restricting OFC's entrance into industrial applications.

Distance measurement based on mode-resolved many-wavelength interferometry realized accurate and long distance measurements with a single frequency comb. This method utilizes mode-resolved OFC to measure distance, which uses the repetition frequency as the ruler. When calculating the distance, dispersion of the OFC can be neglected with the assumption that the group refractive index is wavelength-independent. However, a finer ruler, the wavelength of each OFC modes, can also be used to calculate the distance. In this situation, the assumption is no longer valid. We proposed a compensation method which can improve the result to sub-wavelength level. In order to avoid the ambiguity problem, the mode-resolved method is used as the previous measurement to obtain the final result.

The main reason for expensive measuring system is the complexity and large size of the OFC laser source. An integrated optical frequency comb laser source on a chip is a good solution to reduce the price and size of the setup. In this thesis, We showed a measurement result based on mode-resolved interferometry with an integrated mode-locked laser on a chip. The chip size is smaller than a coin. The tunability of repetition frequency of the OFC allows absolute distance measurement without any other measuring devices. Though the size and cost are extremely reduced by the integrated optics laser, spectral width and coherence of integrated mode-locked laser need to further im-

prove to be able to meet the high-accuracy and long distance demands of industrial and other applications.

Spectrally resolved interferometry is a good method to realize accurate and long distance measurements with a single frequency comb. Virtually imaged phase array (VIPA) spectrometer can absolutely resolve the OFC and the interference pattern can be obtained on a camera. However, the complexity and difficult alignment of VIPA spectrometer limit the further application of this method in the industrial field. In order to solve this problem, We propose a absolute distance measurement method based on spectrally resolved interferometry with a gain-switched dual optical comb. With dual comb system, the interference pattern can be easily obtained with a photodiode detector and low frequency spectrum analyzer. The large range tunability of repetition frequency realizes non-ambiguity arbitrary distance measurement. Though the bandwidth of dual comb needs to be further improved, the simplification and improvements are significant for further industrial applications.

Except the methods mentioned above, we proposed a distance measurement method with frequency sweeping interferometry. When sweeping the frequency with the tunable laser, the interference signal is simultaneously resampled with high finesse Fabry-Perot cavity placed in vacuum, which eliminates the influence of the sweeping nonlinearity. This method successfully obtained a series of interference signals in time domain, which is similar to an optical frequency comb. It provides a cheaper solution for absolute distance measurement without OFC.

In oder to meet the demands of industry and other applications, the cost and size of OFC should be reduced and improved. In this thesis, we demonstrate three solutions with integrated mode-locked laser, dual comb system and frequency sweeping interferometry. The distance is successfully measured with a cheaper and compact measurement systems. Compared to traditional OFC measurement solution, the accuracy needs to be further improved with better properties of the laser.

SAMENVATTING

Lengte is een van de fundamentele fysische grootheden en de precieze meting ervan is erg belangrijk voor wetenschap en technologie. Lasergebaseerde afstandsmeettechniek is een krachtig instrument dat op grote schaal wordt toegepast in geodetische monitoring, omgevingsmonitoring en precisiemeting, ook in ruimtetoepassingen. Sinds de uitvinding van de optische frequentiekam (OFC) aan het begin van deze eeuw, wordt het gebruikt als een veelzijdig hulpmiddel voor vele toepassingen, zoals frequentiemetrologie, spectroscopie, enz. OFC heeft een belangrijke rol gespeeld in afstandsmetrologie, waardoor de ontwikkelde technieken een hoge nauwkeurigheid kunnen bereiken bij langeafstandsmeting. In het tijdsdomein is OFC een pulstrein, die afstand kan meten met de vluchttijdmethode of correlatiedetectiemethode. In het frequentiedomein bestaat het spectrum van OFC uit een reeks discrete lijnen met een gelijk frequentieverschil. Methoden van dispersieve interferometrie, multi-heterodyne interferometrie en multi-golflengte-interferometrie zijn de technieken die worden voorgesteld en gedemonstreerd in spectrale domeinafstandsmetrologie. Hoewel technieken voor afstandsmetrologie op basis van OFC al tientallen jaren zijn ontwikkeld, zijn er nog steeds uitdagingen die moeten worden overwonnen. Bij de meeste toepassingen worden de metingen uitgevoerd in de lucht, waar de resultaten worden beïnvloed door de brekingsindex van lucht. Omdat de OFC een laserbron met meerdere golflengten is, is de brekingsindex van lucht moeilijk te bepalen. De andere uitdaging is de complexiteit en de hoge kosten van het meetsysteem. Tot nu toe is er, voor zover ik weet, geen commerciële afstandsmeter die is gebaseerd op OFC. Het grote formaat, de complexe configuratie en de hoge prijs zijn de bottlenecks die de toegang van OFC tot industriële toepassingen beperken.

Afstandsmeting op basis van mode-resolved veel-golflengte-interferometrie realiseerde nauwkeurige en lange afstandsmetingen met een enkele frequentiekam. Deze methode maakt gebruik van OFC met modusresolutie om afstand te meten, waarbij de herhalingsfrequentie als liniaal wordt gebruikt. Bij het berekenen van de afstand kan de spreiding van de OFC worden verwaarloosd met de aanname dat de groepsbrekingsindex onafhankelijk is van de golflengte. Een fijnere liniaal, de golflengte van elke OFC-modus, kan echter ook worden gebruikt om de afstand te berekenen. In deze situatie is de aanname niet langer geldig. We hebben een compensatiemethode voorgesteld die het resultaat kan verbeteren tot subgolflengteniveau. Om het dubbelzinnigheidsprobleem te vermijden, wordt de mode-resolved-methode gebruikt als de vorige meting om het eindresultaat te verkrijgen.

De belangrijkste reden voor een duur meetsysteem is de complexiteit en het grote formaat van de OFC-laserbron. Een geïntegreerde optische frequentiekamlaserbron op een chip is een goede oplossing om de prijs en omvang van de opstelling te verminderen. In dit proefschrift lieten we een meetresultaat zien op basis van mode-resolved interferometrie met een geïntegreerde mode-locked laser op een chip. De chipgrootte is kleiner dan een munt. De afstembaarheid van de herhalingsfrequentie van de OFC maakt abso-

lute afstandsmeting mogelijk zonder enige andere meetapparatuur. Hoewel de omvang en de kosten extreem worden gereduceerd door de geïntegreerde optische laser, moeten de spectrale breedte en coherentie van de geïntegreerde mode-vergrendelde laser verder worden verbeterd om te kunnen voldoen aan de hoge nauwkeurigheid en lange afstandseisen van industriële en andere toepassingen.

Spectraal opgeloste interferometrie is een goede methode om nauwkeurige en lange-afstandsmetingen te realiseren met een enkele frequentiekam. Virtually Imaged Phase Array (VIPA) spectrometer kan de OFC absoluut oplossen en het interferentiepatroon kan op een camera worden verkregen. De complexiteit en moeilijke uitlijning van de VIPA-spectrometer beperken echter de verdere toepassing van deze methode op industrieel gebied. Om dit probleem op te lossen, stellen we een absolute afstandsmeetmethode voor op basis van spectraal opgeloste interferometrie met een versterkingsgeschakelde dubbele optische kam. Met dubbel kamsysteem, het interferentiepatroon kan eenvoudig worden verkregen met een fotodiodedetector en een laagfrequente spectrumanalysator. De grote afstembaarheid van de herhalingsfrequentie realiseert niet-ambiguïteit willekeurige afstandsmeting. Hoewel de bandbreedte van dubbele kam verder moet worden verbeterd, zijn de vereenvoudiging en verbeteringen significant voor verdere industriële toepassingen.

Behalve de hierboven genoemde methoden, hebben we een methode voor afstandsmeting voorgesteld met frequentie-sweeping interferometrie. Bij het vegen van de frequentie met de afstembare laser, wordt het interferentiesignaal tegelijkertijd opnieuw bemonsterd met de hoge finesse Fabry-Perot-holte die in vacuüm is geplaatst, waardoor de invloed van de vegende niet-lineariteit wordt geëlimineerd. Deze methode heeft met succes een reeks stoorsignalen verkregen in het tijdsdomein, vergelijkbaar met een optische frequentiekam. Het biedt een goedkopere oplossing voor absolute afstandsmeting zonder OFC. s Om aan de eisen van de industrie en andere toepassingen te voldoen, moeten de kosten en omvang van OFC worden verminderd en verbeterd. In dit proefschrift demonstreren we drie oplossingen met geïntegreerde mode-vergrendelde laser, dubbel kam-systeem en frequentie sweeping interferometrie. De afstand wordt met succes gemeten met een goedkoper en compact meetsysteem. In vergelijking met traditionele OFC-meetoplossingen, moet de nauwkeurigheid verder worden verbeterd met betere eigenschappen van de laser.

1

INTRODUCTION

1.1. BACKGROUND: THE EVOLUTION OF OPTICAL FREQUENCY COMB

Since the first laser was constructed by Theodore H. Maiman in 1960, 60 years have elapsed [1]. During this period different types of lasers were invented. Based on the gain medium used to generate the laser they can be classified as gas lasers, chemical lasers, dye lasers, solid-state lasers, semiconductor laser and other types of lasers [2]. All these lasers play an important role in modern society. They are used in businesses, health care, optical sensing, metrology, industrial manufacturing, lithography and communication technology. All these applications benefit from the coherent, directional and monochromatic properties of lasers.

One of the most important kinds of lasers for optical precision metrology is the optical frequency comb (OFC), whose spectrum consists of a series of discrete lines with equal frequency difference. In time domain, it is a train of pulses, whose durations are ultra short and on the order of femtosecond (10^{-15}s) or attosecond (10^{-18}s). This property means that the device can reach very high peak power, which is extremely significant in industrial manufacturing and medical surgery. In frequency domain, the discrete lines resemble a comb. This is why these lasers are called the OFC. Based on the self-referenced phase stabilization technology, which was awarded the Nobel prize in 2005, the frequency of each line is phase-locked and ultrastable. As a result, once the wavelength of a single OFC lines is determined, the others are known. This unique property is beneficial for optical precision metrology.

The traditional way to generate OFC is to use phase-stabilized mode locked laser (MLL), which was first utilized in 1980s [3, 4]. With the development of OFC technology different generation methods have been published over the past 20 years, such as four-wave mixing method [5], with microstructured fiber [6], using microresonator [7] and electro-optic modulation methods [8]. Each method has its benefits, some of them allow the tuning of the repetition frequency [9–11],others are compact [7] and some others more energy efficient [8]. All these methods opened a new era of OFC applications.

They can be used as a powerful tool for distance metrology, optical sensing and medical applications[12–14].

1.2. DISTANCE METROLOGY USING LASERS

Length is one of the seven fundamental physical quantities and its precise measurement is very important for science and technology [15]. The distance metrology is widely applied in geodetic monitoring, environmental monitoring and precision measurement engineering including in space applications. The most direct way to measure absolute distances is time-of-flight method using laser pulses. This method works for long distance measurement [16]. However, the limited electrical bandwidth of the available high-speed photoreceivers would restrict the detection resolution, between the optical pulses, to picoseconds (ps). The latter would limit the detection resolution to the millimeter range [17]. Laser based interferometric techniques overcome this restriction by measuring the phase difference between the interference of light pulses. This method has been used as an important distance measurement tool since it was applied in commercial instruments in 1970s [18]. Initially, a single wavelength laser source, such as He-Ne laser, was used to measure the distance, which led to incremental displacement measurements with sub-wavelength resolution [19]. In order to realise the absolute distance measurement, several principles were proposed, such as the laser intensity modulation [20, 21], light source polarization and frequency modulation [12, 22–24], light source frequency sweeping [25, 26] and multiple-wavelength interferometry [27, 28]. After the development of the OFC laser source, the OFC based measurement methods are becoming more and more important in distance metrology. These techniques will be illustrated in detail in the next chapter.

In order to satisfy the demand of industrial applications, a lot of methods have been published recently. The long distance measurements in air however have a major limitation in accuracy due to the uncertainty of the refractive index of air. Two colour measurement is a good solution to cancel the impact of refractive index [29]. This method makes the measurement result insensitive to the fluctuation of the refractive index, but the determination of the constant value should be further improved. Another major issue is the size and complexity of the laser. The technology of OFC should not only remain in the laboratory but should also find industrial applications. One of the solutions is described in the next section.

1.3. INTEGRATED OPTICS

In most applications the experiments that demonstrate these techniques consist of large setups on experimental optical tables. Applications require devices which can implement dimensional metrology but have a small footprint in terms of size, power consumption and lower cost. These devices could then be used universally to control processes in industry, remote environmental monitoring or flown in satellites.

An integrated mode-locked laser on a chip with a high repetition rate can be the key device which can move this technology from laboratories to industrial and outdoor applications [30]. Ideally this device should have a small footprint in size and power consumption. Additionally this device should be sufficiently isolated so that it remains sta-

ble in spite of variations in its ambient environment.

Several techniques have been published to generate OFC based on integrated optics technology. One is called Kerr combs, which are based on Kerr nonlinearity and consist of a micro-resonator that is pumped by a high power continuous wave laser[31]. Another method is based on monolithically integrated semiconductor mode-locked laser (MML)[32]. The intensity modulation of a CW laser source also allows the generation of an OFC, although the frequency span is limited. All these methods have benefits and drawbacks. This thesis will focus on demonstrating the feasibility and limitations of using the later two laser systems for distance metrology.

1.4. GOAL OF OUR RESEARCH AND THE OUTLINE OF THIS THESIS

In this thesis, we will focus on the distance measurement with OFC. There are two main directions on this topic. One is to improve the measurement accuracy which can be up to 10^{-8}m. The other is to reduce the size of the OFC which is very important for future applications in industry. In this thesis Chapter 3 describes dispersion correction methods which push the mode resolved distance metrology closer to higher accuracies. In Chapter 4 a distance metrology system based on integrated mode locked lasers is described. Chapter 5 is based on a distance metrology system based on a gain switched dual comb laser system. Chapter 6 describes a technique based on a laser system which based on a tunable laser and a Fabry Perot cavity, is used to demonstrate distance metrology. Chapter 7 is the conclusion, discussion and outlook of the research described in this thesis.

REFERENCES

[1] T. H. Maiman, *Stimulated optical radiation in ruby,* nature **187**, 493 (1960).

[2] W. T. Silfvast, *Laser fundamentals cambridge university press,* New York, NY (1996).

[3] J. D. Kafka, M. L. Watts, and J.-W. Pieterse, *Picosecond and femtosecond pulse generation in a regeneratively mode-locked ti: sapphire laser,* IEEE journal of quantum electronics **28**, 2151 (1992).

[4] S. T. Cundiff, *Phase stabilization of ultrashort optical pulses,* Journal of Physics D: Applied Physics **35**, R43 (2002).

[5] G. A. Sefler, *Frequency comb generation by four-wave mixing and the role of fiber dispersion,* Journal of lightwave technology **16**, 1596 (1998).

[6] A. Bartels, R. Gebs, M. S. Kirchner, and S. A. Diddams, *Spectrally resolved optical frequency comb from a self-referenced 5 ghz femtosecond laser,* Optics letters **32**, 2553 (2007).

[7] P. Del'Haye, A. Schliesser, O. Arcizet, T. Wilken, R. Holzwarth, and T. J. Kippenberg, *Optical frequency comb generation from a monolithic microresonator,* Nature **450**, 1214 (2007).

[8] K.-P. Ho and J. M. Kahn, *Optical frequency comb generator using phase modulation in amplified circulating loop,* IEEE photonics technology letters **5**, 721 (1993).

[9] B. R. Washburn, R. W. Fox, N. R. Newbury, J. W. Nicholson, K. Feder, P. S. Westbrook, and C. Jørgensen, *Fiber-laser-based frequency comb with a tunable repetition rate,* Optics Express **12**, 4999 (2004).

[10] A. J. Metcalf, V. Torres-Company, D. E. Leaird, and A. M. Weiner, *High-power broadly tunable electrooptic frequency comb generator,* IEEE Journal of Selected Topics in Quantum Electronics **19**, 231 (2013).

[11] S. Preussler, N. Wenzel, and T. Schneider, *Flat, rectangular frequency comb generation with tunable bandwidth and frequency spacing,* Optics Letters **39**, 1637 (2014).

[12] U. Minoni, L. Rovati, and F. Docchio, *Absolute distance meter based on a frequency-modulated laser diode,* Review of scientific instruments **69**, 3992 (1998).

[13] N. Picqué and T. W. Hänsch, *Frequency comb spectroscopy,* Nature Photonics **13**, 146 (2019).

[14] W. Xia and X. Chen, *Recent developments in fiber-based optical frequency comb and its applications,* Measurement Science and Technology **27**, 041001 (2016).

[15] S. Kononogov, *Fundamental physical constants and systems of units for physical quantities,* Measurement Techniques **50**, 1 (2007).

[16] K. Minoshima and H. Matsumoto, *High-accuracy measurement of 240-m distance in an optical tunnel by use of a compact femtosecond laser,* Applied Optics **39**, 5512 (2000).

[17] Y.-S. Jang and S.-W. Kim, *Distance measurements using mode-locked lasers: a review,* Nanomanufacturing and Metrology **1**, 131 (2018).

[18] N. Bobroff, *Recent advances in displacement measuring interferometry,* Measurement Science and Technology **4**, 907 (1993).

[19] T. Yoon, J. Ye, J. Hall, and J.-M. Chartier, *Absolute frequency measurement of the iodine-stabilized he-ne laser at 633 nm,* Appl. Phys. B **72**, 221 (2001).

[20] K. Froome and R. Bradsell, *Distance measurement by means of a light ray modulated at a microwave frequency,* Journal of scientific instruments **38**, 458 (1961).

[21] I. Fujima, S. Iwasaki, and K. Seta, *High-resolution distance meter using optical intensity modulation at 28 GHz,* Measurement Science and Technology **9**, 1049 (1998).

[22] D. Uttam and B. Culshaw, *Precision time domain reflectometry in optical fiber systems using a frequency modulated continuous wave ranging technique,* Journal of Lightwave Technology **3**, 971 (1985).

[23] T. Kubota, M. Nara, and T. Yoshino, *Interferometer for measuring displacement and distance,* Optics letters **12**, 310 (1987).

[24] A. B. Mateo and Z. W. Barber, *Precision and accuracy testing of fmcw ladar-based length metrology,* Applied optics **54**, 6019 (2015).

[25] H. Kikuta, K. Iwata, and R. Nagata, *Distance measurement by the wavelength shift of laser diode light,* Applied optics **25**, 2976 (1986).

[26] D. Xiaoli and S. Katuo, *High-accuracy absolute distance measurement by means of wavelength scanning heterodyne interferometry,* Measurement Science and Technology **9**, 1031 (1998).

[27] G. BOURDET and A. ORSZAG, *Absolute distance measurements by co2 laser multi-wavelength interferometry,* SPIE milestone series **28**, 213 (1991).

[28] J. A. Stone, A. Stejskal, and L. Howard, *Absolute interferometry with a 670-nm external cavity diode laser,* Applied optics **38**, 5981 (1999).

[29] K. Minoshima, K. Arai, and H. Inaba, *High-accuracy self-correction of refractive index of air using two-color interferometry of optical frequency combs,* Optics Express **19**, 26095 (2011).

[30] K. Hei, G. Shi, A. Hänsel, Z. Deng, S. Latkowski, S. A. Van den Berg, E. Bente, and N. Bhattacharya, *Distance metrology with integrated mode-locked ring laser,* IEEE Photonics Journal **11**, 1 (2019).

[31] V. Brasch, E. Lucas, J. D. Jost, M. Geiselmann, and T. J. Kippenberg, *Self-referenced photonic chip soliton kerr frequency comb,* Light: Science & Applications **6**, e16202 (2017).

[32] A. Matsko, A. Savchenkov, W. Liang, V. Ilchenko, D. Seidel, and L. Maleki, *Mode-locked kerr frequency combs,* Optics letters **36**, 2845 (2011).

2

DISTANCE MEASUREMENT INTERFEROMETRY USING FREQUENCY COMB

The most direct method to estimate distances is using time of flight with laser pulses. Higher accuracies are achieved using interferometry where the phase difference is extracted from the interfering light. The measurements of interference can be done using different optical interferometer setups like Mach Zehnder, Michelson, Sagnac or Twyman Green. It is only after the arrival of the optical frequency comb (OFC) that interference between laser pulses for interferometry became commonplace. A myriad of techniques using the OFC have been proposed and demonstated. This chapter introduces the state of art of these techniques.

2.1. OPTICAL FREQUENCY COMB

Since the optical frequency comb (OFC) was invented at the beginning of the century[1], it has become one of the most important tools for many applications, such as distance metrology [2, 3], spectroscopy [4] and optical communication [5].

As illustrated in Fig. 2.1, OFC in the time domain can be seen as a train of ultra-short pulses with a spacing of T_r between them. The pulse duration is on the order of hundreds or tens of femtoseconds. In the spectral domain, OFC consists of a series of discrete, equally spaced frequency lines with a mode spacing of f_{rep}, which seems like a comb. Therefore it gets the name "Frequency comb". The optical frequency of the i^{th} mode can be expressed as $f_i = i \times f_{rep} + f_o$ with f_o denoting the carrier-envelope offset frequency. The carrier-envelope offset frequency is caused by the dispersion in the laser cavity, which causes the difference between the phase and group velocity. In time domain, the carrier phase of the pulses will periodically change relative to the carrier envelope phase. The phase difference of the carrier and the envelope between adjacent

pulses is ϕ_{ceo}. In spectral domain, this difference is reflected in f_o, which means the initial offset frequency relative to zero frequency.

OFC can be generated by several methods, including amplitude or phase modulation of a continuous-wave laser, four-wave mixing in nonlinear media, or stabilization of the pulse train generated by a mode-locked laser. Different kinds of OFC lasers were invented based on these techniques, such as mode-locked Ti:Sapphire laser[6], mode-locked Erbium-doped fiber laser[7], Yb fiber laser [8], electro-optic frequency comb [9] and Kerr frequency comb [10].

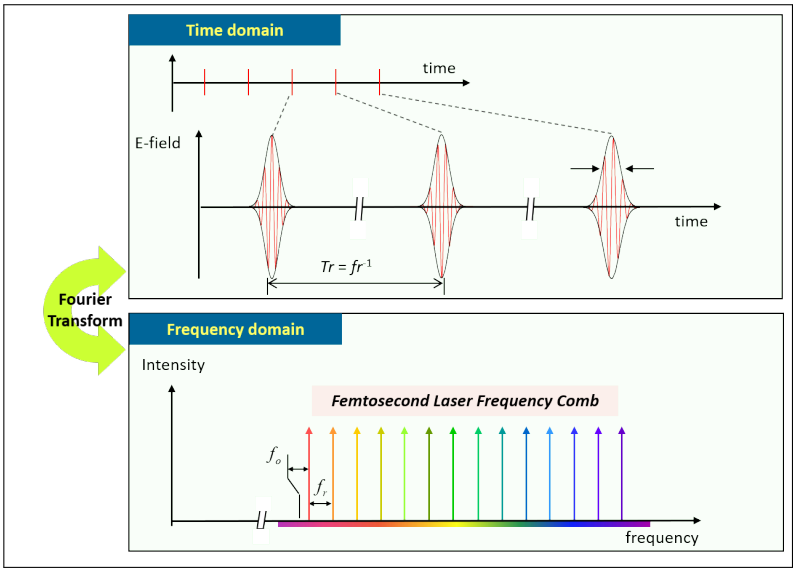

Figure 2.1: Temporal and spectral characteristics of mode-locked lasers. In time domain OFC is a train of pulses and in frequency domain it appears to be a comb. The time domain signal can be easily converted to frequency domain using a Fourier transform.

2.2. DISTANCE MEASUREMENT USING CORRELATION

The method based on pulse correlation to measure the distance was proposed by Ye in 2004 [11]. The main idea is to obtain the cross correlation of two coherent pulses using Michelson interferometer. The typical setup is shown in Fig. 2.2. The light is split into a part going to the reference arm and the other part going to the measurement arm, by the beam splitter. In the reference arm the retroreflector was mounted on a piezo-electric transducer (PZT), which is used to generate displacement. In the measurement arm the beam propagates for a long distance and is reflected by another retroreflector. The reflected light is overlapped and detected by a photodetector. At the initial position, the first correlation pattern is observed by scanning the reference arm. The reflector mounted on the mechanical car in the measurement arm is then moved to an arbitrary distance. The reference arm is scanned again to obtain the second correlation pattern. The L, the displacement of the measurement arm, can be obtained from

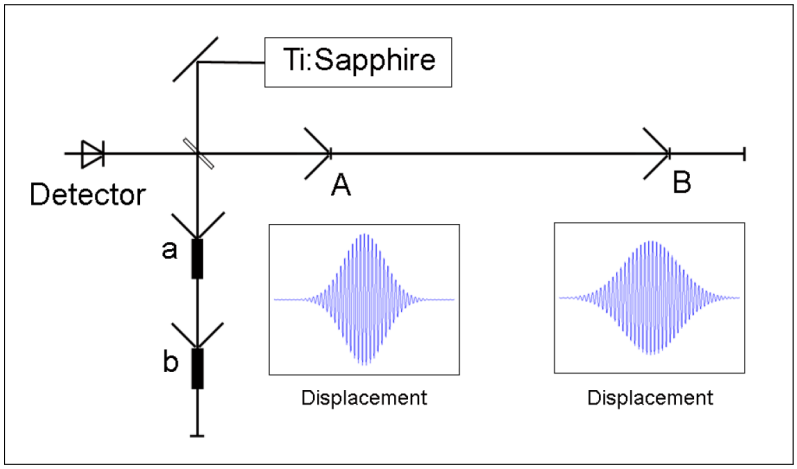

Figure 2.2: The schematic of a typical experimental setup for distance measurement using pulse correlations.

$$L = N \times L_{pp} + \Delta L. \tag{2.1}$$

Here, N is an integer number and ΔL is the displacement of the reference arm. L_{pp} is the pulse-to-pulse distance in the medium, which is written as:

$$L_{pp} = \frac{c}{f_{rep} n_g}. \tag{2.2}$$

with n_g the group refractive index and f_{rep} the repetition frequency of the frequency comb. The integer number N can be determined with tuning the f_{rep} or other methods, with an accuracy better than half of the L_{pp}. There are several methods to determine the ΔL, such as measuring peak position [11, 12] or measuring the movement of the peak position [13, 14]. These methods can realise high accuracy long distance measurement. However, the measurement speed and complexity of the set up are limited by the mechanical translation stages of the system.

2.3. MULTI-WAVELENGTH INTERFEROMETER

In order to realise the absolute distance measurement, a multi-wavelength laser source is used. However, maintaining the stabilization of the wavelength is the key problem in implementing high accuracy measurement. OFC provides a good solution to this since individual single wavelength lasers can be phase-locked to the modes of the reference frequency comb generating an accurate multi wavelength source. The concept of the generation of four wavelengths phase-locked to the frequency comb for multi-wavelength interferometry is demonstrated in [15]. The distance to be measured L_i calculated by different wavelengths λ_i can be described as:

$$L_i = \frac{\lambda_i}{n_i}(m_i + e_i). \tag{2.3}$$

Here, n_i is the refractive index of air, m_i is an integer number and e_i is a fraction and can be extracted from the interference signal. To determine m_i, an optimization of $|L - L_i|$ for all λ_i is minimized through a sequence of numerical iterations. The accuracy of this method can achieve sub-wavelength level. In air the uncertainty is estimated to be at the level of 10^{-8}, which is limited by the determination of the refractive index. In vacuum it can achieve accuracies of 10^{-10}.

The OFC is thus a very stable reference source for generating many accurate wavelength sources. However, the phase-locked setup is very complex, especially for more than two different wavelengths. For the applications in industry, the cost and size of the measurement instruments are very important. Therefore this method needs to be further improved to fulfil the demand of applications.

2.4. SPECTRAL DOMAIN FREQUENCY COMB INTERFEROMETRY

2.4.1. FREQUENCY COMB INTERFEROMETER WITH GRATING

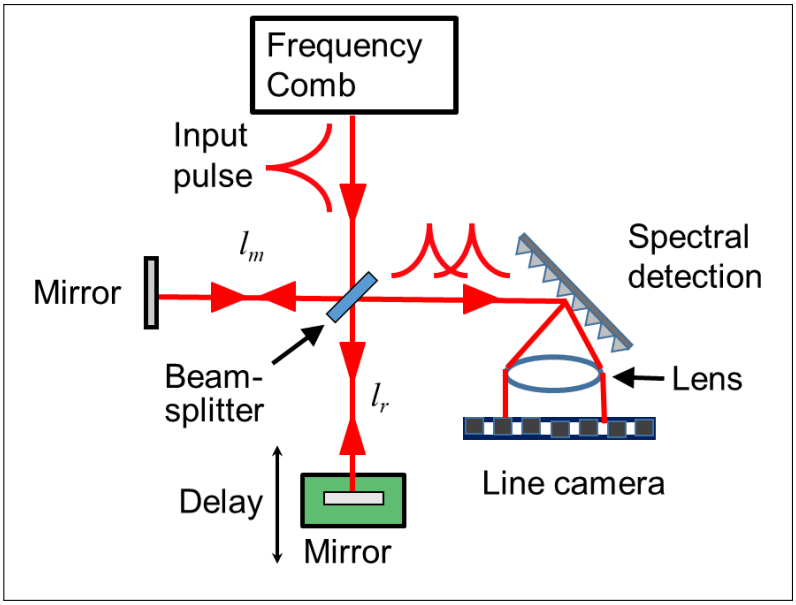

Figure 2.3: The setup of frequency comb interferometer with grating.

As shown in Fig. 2.1, in the spectrum domain OFC can be seen as a many-wavelength laser source with thousands of different wavelengths. If there is a method to spectrally disperse the modes of the OFC, the distance can be easily achieved by using the interference phase information of all modes. An initial setup of spectral interferometry method is illustrated in Fig. 2.3. A Ti:sapphire mode-locked pulse laser, emitting 10 fs ultrashort pulses at a repetition rate of 75 MHz, was used as the laser source. A typical Michelson interferometer is used to obtain the interference signal of the measurement and reference arm. The interference signal is recorded by a line CCD camera. A typically data proce-

dure is shown in Fig. 2.4. At first we obtain the modulated interference signal captured by the camera. Hereafter the DC signal is filtered out by a Fourier band-pass filter. The phase can be extracted from the real part and image part of the signal. After unwrapping the phase ϕ, the distance L can be described as:

$$L = \frac{d\phi}{df}\frac{c}{4\pi n_g}. \tag{2.4}$$

Here, n_g is the group refractive index and c is the speed of light in vacuum.

This method successfully measures the distance with dispersed OFC. The experiment result demonstrates a non-ambiguity range of 1.46 mm with a resolution of 7 nm. This method was also demonstrated to be suitable for long distance measurement [16].

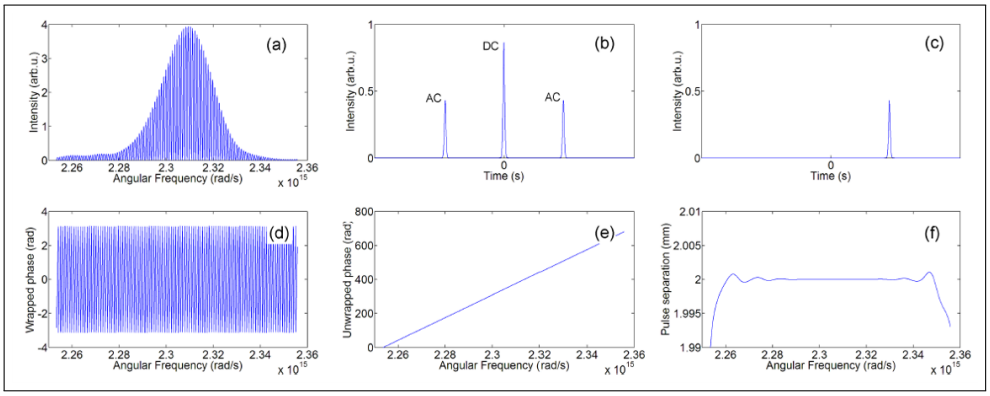

Figure 2.4: Data processing procedure for measurement of L[16]. (a) The spectral interferogram i.e. dispersed interference intensity captured by the line CCD. (b) Fourier transform of the measured spectral interferogram. (c) The DC peak and one AC peak are band pass filtered. (d) The wrapped phase. (e) The unwrapped phase. (f) The pulse separation obtained from the derivative of the unwrapped phase.

2.4.2. SPECTRALLY RESOLVED FREQUENCY COMB INTERFEROMETER WITH VIRTUALLY IMAGED PHASE ARRAY

In order to fully resolve the OFC, virtually imaged phase array (VIPA) is used to improve the interferometer [3]. The typical setup of VIPA spectrometer is demonstrated in Fig. 2.5. In the spectrometer the combination of cylindrical lens and VIPA etalon are used as an angular disperser, which results in wavelength-dependent transmission for different angles. Due to the free spectral range of VIPA the modes of OFC are overlapped in vertical line. Therefore a grating is used to expand the modes in horizontal direction. Finally a focusing lens is applied to image all the modes on the CCD camera. The image of resolved modes by camera is also shown in Fig. 2.5.

In order to measure distance, the VIPA spectrometer as shown in Fig. 2.5 replaces the line camera based spectrometer in Fig. 2.3 in the detection arm of the Michelson interferometer. Also a fringe counting He-Ne laser is co-propagated with the frequency comb beam and used as the gold standard measurement. The data processing procedures are similar as the method mentioned above. With the modulated interference signal the

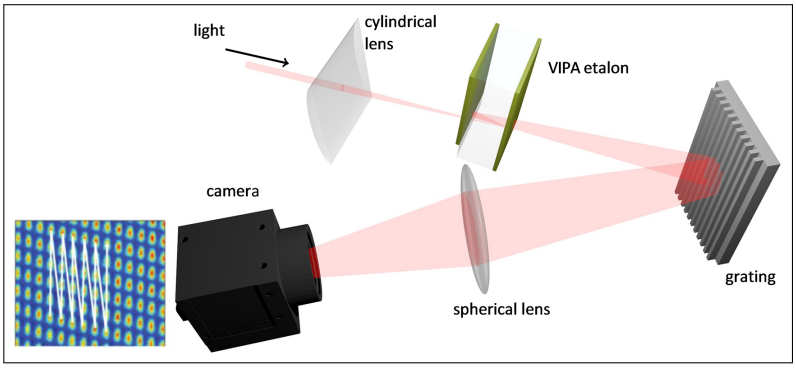

Figure 2.5: High-resolution spectrometer based on a VIPA and a grating for analysis of the frequency comb spectrum[17].

phase information can be extracted by normalization method. The distance L can be obtained by:

$$L = \frac{C}{f_{rep}} \frac{c}{4\pi n_g}. \tag{2.5}$$

with C the derivative of the phase with respect to the frequency of the modes, L the path length difference of the interferometer arms (single path), f_{rep} the repetition frequency, c the speed of light in vacuum, and n_g the group refractive index.

The accuracy of this method can be up to sub-wavelength level. However, it can not measure arbitrary distance. When the distance is near to an integer multiple of the pulse-to-pulse distance L_{pp}, the determination of C will be difficult and inaccurate. For arbitrary long distance measurement it needs other methods to complete the previous measurement of distance, which means it is not an absolute arbitrary distance method.

2.5. DUAL-COMB INTERFEROMETRY

The single-comb-based distance measurement methods mentioned above realise the measurement with high accuracy. However, in order to extract the phase information of OFC several complex components are used, which increases the complexity of the system and limits the further application in industry. As the development of integrated optics technology the dual comb measurement system (DCMS) becomes more and more attractive for distance metrology. The typical setup of DCMS is shown in Fig. 2.6. Here the photodiode captures the interference signal between two frequency combs with slightly different f_{rep}. The spectral interferogram can be low-pass filtered to a frequency comb in the RF domain which contain the phase and amplitude informetion. The dual comb technique has been also applied to spectroscopy [18–20], hyperspectral imaging [21, 22], microscopy [23], vibrometry [24], and strain sensors [25].

The dual comb method is similar as the sampling method which is called equivalent-time sampling. The Nyquist Theorem states that in order to adequately reproduce a signal it should be periodically sampled at a rate that is 2 times the highest frequency you wish to record. In order to realise better quality of reproduced signal, the sample

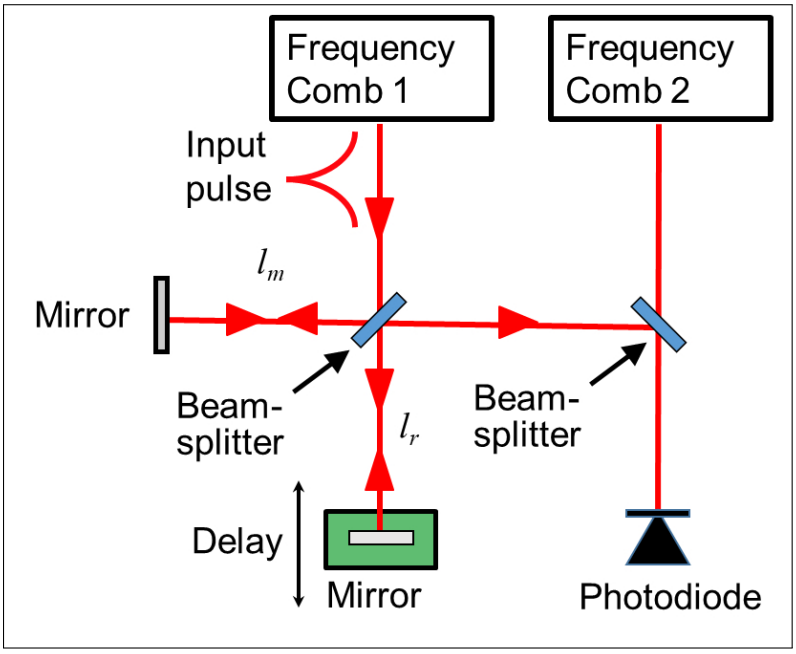

Figure 2.6: Typical setup of DCMS. Comb1 generates the signal comb, which go through a Michelson interferometer. Then the interference pulses are sampled by Comb2 which has a slightly different repetition frequency.

rate should be even higher than Nyquist frequency. For OFC, of which pulse duration is in femtosecond level, it is difficult to sample the pulses in real-time. This makes the equivalent-time sampling a good solution for measuring using the OFC. When sampling a single period signal, the real-time method obtains the sampling points in one period. However, we can also get one point in one period and sample several periods, as long as the sampling frequency is slightly different from the signal frequency. Then the sampling rate is dramatically decreased by this method.

Signal pulses (repetition time T_{r1}) combined with reference and measurement pulses are sampled by a LO pulses (repetition time T_{r2}) which have different repetition rates from the signal pulse. In each period, the LO pulse shifts $\Delta T = (T_{r2}\text{-}T_{r1})$ relative to the signal pulses, and samples a slightly different portion of the signal. The updated time (T_{update}), which is the minimal sampling time to obtain the fully interferogram, is described as:

$$T_{update} = \frac{T_{r1}^2}{\Delta T}. \tag{2.6}$$

Based on the equivalent time sampling theory, the relation between Δt, which is determined by the peaks of the fitted envelopes, and $\Delta\tau$, which is the time delay related to the distance difference between the reference and measurment arms, can be described as:

$$\Delta\tau = \frac{\Delta T}{T_{r1}^2}\Delta t. \tag{2.7}$$

The distance can then be obtained from the time delay, expressed as follows:

$$L = \frac{c\Delta\tau}{2} \tag{2.8}$$

where c is the speed of light.

The analysis of the interference signal in the frequency domain can be seen as a multi-heterodyne interferometer. The interference signal which is a radio frequency (RF) signal consists of many heterodyne beats. In order to avoid aliasing, the frequency difference Δf should be satisfied for $\Delta f < \frac{f_{r2}}{2m}$, where m is the number of modes of Comb 2. The phase of the reference and measurement interferograms can be extracted from the intensity recorded by the photo-detector. After obtaining the phase difference between the reference and measurement interferograms, the distance calculation procedures are same as the spectral methods described above.

2.6. REFRACTIVE INDEX IN THE AIR

In most distance metrology applications, these measurements are completed in air. When using interferometers, the wavelength of light in air λ_{air} should be determined first. It is described as:

$$\lambda_{air} = \frac{\lambda_{vac}}{n_{air}}, \tag{2.9}$$

with λ_{vac} the wavelength of light in vacuum and n_{air} the refractive index in the air which describes how fast light travels through the air. Two basic methods for calculating the refractive index are available, an equation developed by Ciddor [26] and an updated version of the Edlén Equation [27] as modified by Birch and Downs. There is only a small difference between the two equations, which can be ignored in most applications [28]. The details of the two equations are shown in Appendix A.

When using OFC to measure the distance, we also need to consider the refractive index. As OFC is a multi-wavelength laser source, in most cases we use group refractive index to do the calculation [3, 29]. Only when the dispersion is considered in the measurement, the refractive index is needed to be calculated separately based on the wavelength, which is discussed in chapter 3.

REFERENCES

[1] R. Holzwarth, T. Udem, T. W. Hänsch, J. Knight, W. Wadsworth, and P. S. J. Russell, *Optical frequency synthesizer for precision spectroscopy,* Physical review letters **85**, 2264 (2000).

[2] U. Minoni, L. Rovati, and F. Docchio, *Absolute distance meter based on a frequency-modulated laser diode,* Review of scientific instruments **69**, 3992 (1998).

[3] S. A. van den Berg, S. T. Persijn, G. J. P. Kok, M. G. Zeitouny, and N. Bhattacharya, *Many-wavelength interferometry with thousands of lasers for absolute distance measurement,* Physical Review Letters **108** (2012), 10.1103/physrevlett.108.183901.

[4] N. Picqué and T. W. Hänsch, *Frequency comb spectroscopy,* Nature Photonics **13**, 146 (2019).

[5] V. Torres-Company and A. M. Weiner, *Optical frequency comb technology for ultra-broadband radio-frequency photonics,* Laser & Photonics Reviews **8**, 368 (2014).

[6] D. J. Jones, S. A. Diddams, J. K. Ranka, A. Stentz, R. S. Windeler, J. L. Hall, and S. T. Cundiff, *Carrier-envelope phase control of femtosecond mode-locked lasers and direct optical frequency synthesis,* Science **288**, 635 (2000).

[7] J. Rauschenberger, T. M. Fortier, D. J. Jones, J. Ye, and S. T. Cundiff, *Control of the frequency comb from a mode-locked erbium-doped fiber laser,* Optics Express **10**, 1404 (2002).

[8] A. Ruehl, A. Marcinkevicius, M. E. Fermann, and I. Hartl, *80 w, 120 fs yb-fiber frequency comb,* Optics letters **35**, 3015 (2010).

[9] J. Lancis, P. Andrés, *et al.*, *Lossless equalization of frequency combs,* Optics letters **33**, 1822 (2008).

[10] P. Del'Haye, A. Schliesser, O. Arcizet, T. Wilken, R. Holzwarth, and T. J. Kippenberg, *Optical frequency comb generation from a monolithic microresonator,* Nature **450**, 1214 (2007).

[11] J. Ye, *Absolute measurement of a long, arbitrary distance to less than an optical fringe,* Opt. Letters **29**, 1153 (2004).

[12] M. Cui, M. G. Zeitouny, N. Bhattacharya, S. A. van den Berg, H. P. Urbach, and J. J. M. Braat, *High-accuracy long-distance measurements in air with a frequency comb laser,* Opt. Letters **34**, 1982 (2009).

[13] H. Matsumoto, X. Wang, K. Takamasu, and T. Aoto, *Absolute measurement of baselines up to 403 m using heterodyne temporal coherence interferometer with optical frequency comb,* Applied Physics Express **5**, 046601 (2012).

[14] X. Wang, S. Takahashi, K. Takamasu, and H. Matsumoto, *Spatial positioning measurements up to 150 m using temporal coherence of optical frequency comb,* Precision Engineering **37**, 635 (2013).

[15] Y.-S. Jang, G. Wang, S. Hyun, H. J. Kang, B. J. Chun, Y.-J. Kim, and S.-W. Kim, *Comb-referenced laser distance interferometer for industrial nanotechnology,* Scientific reports **6**, 1 (2016).

[16] M. Cui, M. G. Zeitouny, N. Bhattacharya, S. A. van den Berg, and H. P. Urbach, *Long distance measurement with femtosecond pulses using a dispersive interferometer,* Opt. Express **19**, 6549 (2011).

[17] S. A. van den Berg, S. van Eldik, and N. Bhattacharya, *Mode-resolved frequency comb interferometry for high-accuracy long distance measurement,* Scientific Reports **5**, 14661 (2015), article.

[18] I. Coddington, N. Newbury, and W. Swann, *Dual-comb spectroscopy,* Optica **3**, 414 (2016).

[19] I. Coddington, W. Swann, and N. Newbury, *Coherent dual-comb spectroscopy at high signal-to-noise ratio,* Physical Review A **82**, 043817 (2010).

[20] S. M. Link, D. J. Maas, D. Waldburger, and U. Keller, *Dual-comb spectroscopy of water vapor with a free-running semiconductor disk laser,* Science **356**, 1164 (2017).

[21] S. Boudreau, S. Levasseur, C. Perilla, S. Roy, and J. Genest, *Chemical detection with hyperspectral lidar using dual frequency combs,* Optics Express **21**, 7411 (2013).

[22] K. Shibuya, T. Minamikawa, Y. Mizutani, H. Yamamoto, K. Minoshima, T. Yasui, and T. Iwata, *Scan-less hyperspectral dual-comb single-pixel-imaging in both amplitude and phase,* Optics Express **25**, 21947 (2017).

[23] E. Hase, T. Minamikawa, T. Mizuno, S. Miyamoto, R. Ichikawa, Y.-D. Hsieh, K. Shibuya, K. Sato, Y. Nakajima, A. Asahara, *et al.*, *Scan-less confocal phase imaging based on dual-comb microscopy,* Optica **5**, 634 (2018).

[24] E. L. Teleanu, V. Durán, *et al.*, *Electro-optic dual-comb interferometer for high-speed vibrometry,* Optics Express **25**, 16427 (2017).

[25] N. Kuse, A. Ozawa, and Y. Kobayashi, *Static fbg strain sensor with high resolution and large dynamic range by dual-comb spectroscopy,* Optics Express **21**, 11141 (2013).

[26] P. E. Ciddor, *Refractive index of air: new equations for the visible and near infrared,* Applied optics **35**, 1566 (1996).

[27] K. Birch and M. Downs, *An updated Edlén equation for the refractive index of air,* Metrologia **30**, 155 (1993).

[28] J. A. Stone Jr and J. H. Zimmerman, *Index of refraction of air*, Tech. Rep. (2001).

[29] K.-N. Joo and S.-W. Kim, *Absolute distance measurement by dispersive interferometry using a femtosecond pulse laser,* Optics Express **14**, 5954 (2006).

3

DISPERSION CORRECTION IN HIGH-ACCURACY LONG DISTANCE MEASUREMENTS BASED ON MODE-RESOLVED FREQUENCY COMB

Mode-resolved frequency comb interferometry is a technique that has demonstrated its ability for high-accuracy distance metrology. In this chapter we propose a dispersion correction modality for distance metrology based on mode-resolved frequency comb interferometry. The dispersion of the group refractive index when determined and compensated adds to the accuracy of the results. Our results show an agreement within 500 *nm for distances up to 50 metres when compared to a conventional fringe counting interferometer.*

3.1. INTRODUCTION

The arrival of the femtosecond frequency comb [1], has provided the field of distance metrology with a new tool. The modes of the laser can be phase-locked to a stable frequency reference such as maser or an atomic clock [2], which makes it possible to use that frequency comb as a ruler for distance measurement with direct traceability to time standard [3]. Frequency comb can be used as a reference for multi-wavelength interferometry, which phase-locks each wavelength individually to frequency comb[4, 5]. The frequency comb can be used as a light source for distance measurement directly. The first measurement reported was based on the phase measurement of the intermode

A manuscript based on the work presented here is in preparation to be submitted to a peer-reviewed scientific journal.

beats of the frequency comb [6]. Cross correlation measurements based on pulse interference in a Michelson interferometer came thereafter [7, 8]. Many other techniques were proposed and demonstrated subsequently such as such as dispersive interferometry [9–12], time-of-flight measurement [13] and dual comb interferometry [14–16].

Distance measurement based on mode-resolved many-wavelength interferometry realized accurate and non-ambiguous measurements with a single frequency comb [11, 12]. For this, the frequency comb is used as many wavelength laser source input into a Michelson interferometer. All the individual modes of the two arms superpose and interfere with each other, and the interference pattern is then spectrally resolved by a virtually imaged phase array (VIPA) spectrometer. The distance is obtained by unravelling the pattern and extracting the phase changes from the interference. However, in this method there is an assumption that the group refractive index is wavelength-independent, which decreases the measurement accuracy of this method. To obtain a more accurate measurement result, dispersion of group refractive index should be properly determined and compensated.

In this chapter we demonstrate a dispersion correction method based on mode-resolved frequency comb. This is a refinement of experiment data that have previously been published in [12]. Together with the measurement based on spectral interferometry, this method can achieve sub-wavelength accuracy.

3.2. MEASUREMENT PRINCIPLES

An optical frequency comb is a pulsed laser whose modes are distributed equally with a mode spacing of frequency f_{rep} and the carrier-envelop offset frequency f_0. The f_{rep} and f_0 are phase-locked to a reference clock. The stabilization of f_{rep} and f_0 allows to measure distance with spectral interferometry and dispersion correction method.

The principle of dispersion correction method proposed in this chapter is based on a Michelson interferometer and a VIPA (Virtually Imaged Phased Array) spectrometer[17, 18].

3.2.1. EXPERIMENTAL SETUP

The setup for the experiment presented in this work has three main components: a frequency comb source, a Michelson interferometer, and a VIPA spectrometer. The frequency comb is generated by a Ti:Sapphire laser,which operates at a repetition frequency of 1.012 GHz. About 6000 modes from 813 nm to 827 nm are used for the measurement. A schematic of the setup is shown in Figure 3.1.

In order to identify the wavelength of individual modes, a tunable single-mode distributed feedback (DFB) diode laser, operating around 817 nm, was coupled into the same fiber which delivers the light of frequency to the system. In parallel, the wavelength of the DFB-laser is measured with a wavemeter with an absolute accuracy of several tens of MHz. With the tunable laser, a known frequency reference dot is recorded by CCD camera. Based on the reference dot and the values of f_{rep} and f_0, the absolute wavelength of each dot can be determined.

The measurement arm of the Michelson interferometer can be changed over a distance of 50 m with an electric carriage carrying the retroreflector. For each measurement

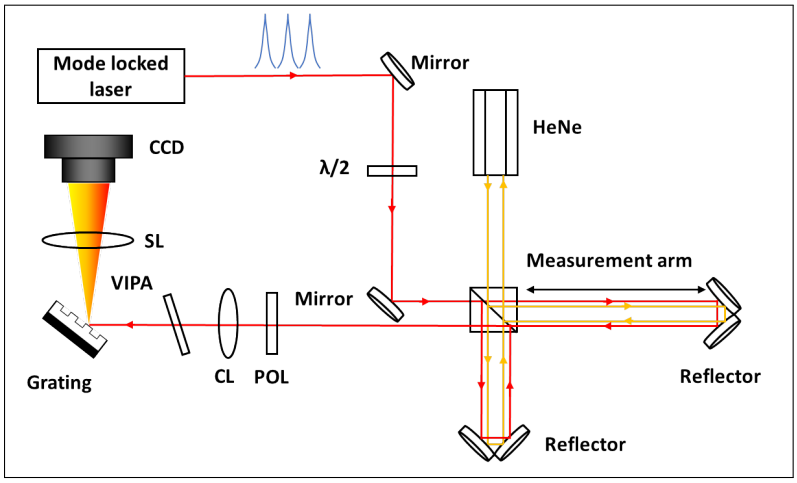

Figure 3.1: Schematic over view of the measurement setup [12].The comb light is delivered to the setup with a single mode (SM) fiber, providing a clean mode profile. Both the HeNe laser (orange line) and comb laser (red line) measure the displacement quasi-simultaneously. PBS: polarizing beam splitter, POL: polarizer, $\lambda/2$: half-waveplate, CCD: charge-coupled device camera, M: planar mirror, RR: hollow retro reflector, CL: cylindrical lens (100 mm focal length), SL: spherical lens (400 mm focal length) .

point the reading of the counting interferometer and frequency comb measurement are compared. Both measurements are performed quasi-simultaneously.

3.2.2. SPECTRAL INTERFEROMETRY

In order to obtain normalized spectrally resolved interference intensity, images of the reference arm and the measurement arm and the interference image are recorded separately by camera. A typical set of recorded images and intensity extracted from these images are shown in Fig. 3.2(a). The DC signal of the interference intensity, which is modulated by VIPA, can be easily removed by substracting the intensity of reference arm and measurement arm. Then the envelop is cancelled by using Hilbert transform [19]. The normalized interference intensity can be written as:

$$I(\phi) = \cos\phi, \quad \phi = \frac{4\pi L f n}{c}, \tag{3.1}$$

with ϕ the phase difference between reference arm and measurement arm, L the path length difference of the interferometer arms (single path), f the optical frequency, c the speed of light in vacuum, and n the refractive index of air. A typically normalized intensity of interference is shown in Fig. 3.2(b).

The derivative of phase with respect to frequency can be written as:

$$\frac{d\phi}{df} = \frac{4\pi L}{c}[n + f\frac{dn}{df}] = \frac{4\pi L}{c}[n_g], \tag{3.2}$$

with n_g the group refractive index. This can be written as:

$$n_g = n - \lambda \frac{dn}{d\lambda} = n + f \frac{dn}{df}. \tag{3.3}$$

The distance then becomes:

$$L = \frac{d\phi}{df} \frac{c}{4\pi n_g}. \tag{3.4}$$

The phase change with frequency is obtained from a cosine fitting result with $\phi = C \cdot p + D$ and n_g the group refractive index,as illustrated in Fig. 3.2(c) . Here n_g is assumed to be wavelength-independent, which has been demonstrated by [12]. C and D are fitting parameters and p is a label related to a specific mode : $f_p = f_{rep}(Q + p) + f_0$, with Q is a very large integer. This leads to

$$L = \frac{C}{f_{rep}} \frac{c}{4\pi n_g}. \tag{3.5}$$

Only cosine fit cannot be enough to determine the C, because we don't know the sign of C. But it is easy to use other methods to obtain it, such as moving the reference arm a little bit or changing the f_{rep}.

Within $\frac{1}{2}L_{pp}$ the distance L is defined without ambiguity. Here L_{pp}, the pulse-to-pulse distance in the medium, is written as :

$$L_{pp} = \frac{c}{f_{rep} n_g}. \tag{3.6}$$

When L is larger than $\frac{1}{2}L_{pp}$, the interference patterns repeat for each $\frac{1}{2}L_{pp}$. The phase change is more than 2π when $L > \frac{1}{2}L_{pp}$, but the cosine fit method only gives phase change which is less than 2π. The arbitrary distance can be written as:

$$L_t = \frac{2\pi m + C}{f_{rep}} \frac{c}{4\pi n_g} = \frac{1}{2} m L_{pp} + L, \tag{3.7}$$

where m is an integer. In our case $L_{pp} \approx$ 30cm, it is easy to find a measurement method of which accuracy is better than $\frac{1}{2}L_{pp}$ and combine with our method to measure distance larger than $\frac{1}{2}L_{pp}$.

3.2.3. DISPERSION CORRECTION

The spectral interferometry method demonstrated above is based on the assumption that n_g is wavelength-independent which is used to simplify the calculation. However, to obtain high accuracy result the dispersion of refractive index should be calculated accurately using its wavelength-dependence property. In this section we will demonstrate an improved spectral interferometry method based on dispersion correction.

In order to correct dispersion, the first step is to determine frequency of each frequency comb mode. The frequency can be described as $f_p = N \cdot f_{rep} + f_0$, with N is a very large integer. As f_{rep} and f_0 known already, we used a single mode laser to be a reference to determine N. The wavelength of single mode laser can be measured with a wavemeter with a high accuracy. The image of spectrally resolved comb and single

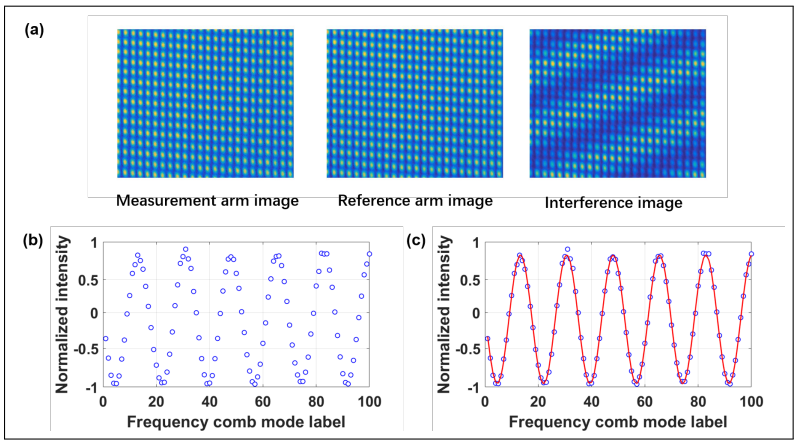

Figure 3.2: Data processing procedure of spectral interferometry; (a) images of measurement arm and reference arm and interference image recorded by camera, (b) the normalized interference intensity extracted from images and (c) cosine fitting result.

mode laser is shown on Fig. 3.3(a). Based on the values of N, f_{rep} and f_0, the absolute wavelength of each mode can be determined.

Based on the accurate frequency of each mode and environmental conditions (air temperature, pressure and humidity), the refractive index n_p can be calculated with the Edlén equation [20]. The normalized intensity can be determined again with the frequency f_p and distance L_t:

$$I_p = \cos \frac{4\pi L_t f_p n_p}{c}. \tag{3.8}$$

Fig. 3.3 (b) shows the comparison between the normalized intensity based on Eq. 3.8 and the normalized result after Hilbert transform. The difference of two curves can be seen clearly, which is mainly caused by inaccurate determination of the distance L_t. Using the frequency and refractive index of each mode determined from the calibration images (Fig. 3.3 (b)) and the environmental parameters, we can obtain a normalised intensity curve for an arbitrary distance using Eq. 3.1. Then we compare it with the result of the Hilbert transform on the intensities obtained from the measurement and using Eq. 3.8 to obtain the optimised distance. The optimised distance L_o can be determined by

$$L_o = \min_{L_o} \sum_{\lambda=\lambda_b}^{\lambda_e} |I_p(L_o,\lambda) - I_n(\lambda)|^2, L_t - \frac{1}{4}\lambda_c < L_o < L_t + \frac{1}{4}\lambda_c. \tag{3.9}$$

Here λ_c the central wavelength of frequency comb,λ_b the wavelength first mode,λ_e the wavelength of last mode and $I_n(\lambda)$ normalized intensities obtained from images. The limitation of the range of L_o is to make sure the uniqueness of the optimization result. The optimized result was shown in Fig. 3.3 (c).

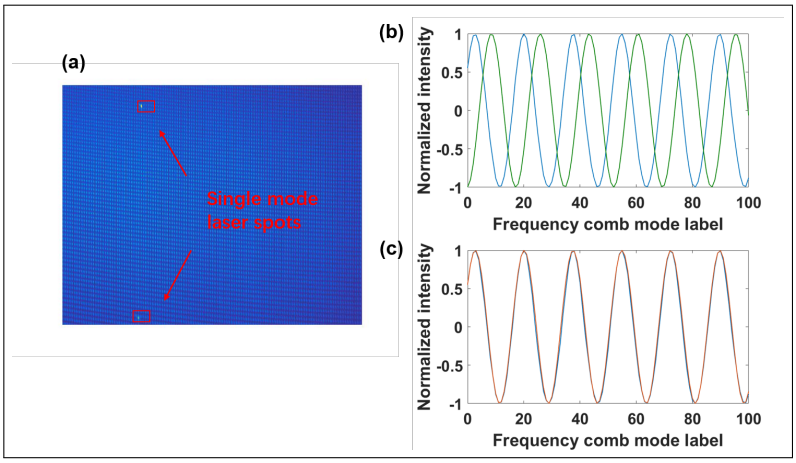

Figure 3.3: Data processing procedure of dispersion correction; (a) image of spectrally resolved frequency comb and single mode laser recorded by camera, (b) comparison between the normalized intensity based on absolute frequency of modes (green) and the normalized result after Hilbert transform (blue) and (c) optimized intensity (red) and the normalized result after Hilbert transform (blue).

3.3. RESULTS AND DISCUSSION

In the experiment, the distances were measured simultaneously with our method and a fringe counting HeNe interferometer for comparison. Firstly, the carriage was positioned at the distance which is similar to reference arm (around 100 µm), and then it is moved to 5 mm.This procedure was repeated for other distances, from 5 m to 50 m in steps of 5 m. The distances were chosen arbitrarily, but the distances close to 0 and $\frac{1}{2}L_{pp}$ were avoided. Because at these distances the fitting results were not accurate enough for dispersion correction. For each position, five measurements with the frequency comb and five measurements of the fringe counting HeNe interferometer were recorded. The environmental conditions(temperature, air pressure and humidity) were recorded simultaneously, which were used for refractive index calculation.

To be able to use the cosine fit, intensity should be normalized. Therefore, the images of reference and measurement arm were recorded individually. A typically normalized intensity based on Hilbert transform are shown in Fig. 3.4 (a) as the blue curve. To clearly show the result, only 100 points of 6000 modes were included in the figure. The green curve is the intensity calculated with Eq. 3.1 based on the distance obtained from the spectral interferometry method and the refractive index for each mode. It is clear to see the mismatch between these two curves. The main reason for the mismatch is the fitting error which comes from ignoring the dispersion of refractive index and the noise of the measurement system. To improve the accuracy of the measurement result, the dispersion correction method is used to remove the fitting error from the results obtained by the spectral interfermetry method. The result of this method is shown in Fig. 3.4 (b). The blue curve is also the normalized intensity and the red curve is the corrected result based on the distance optimized with Eq. 3.8. After correction, the two curves match very well. The difference between the normalized intensity and the optimized result is shown in

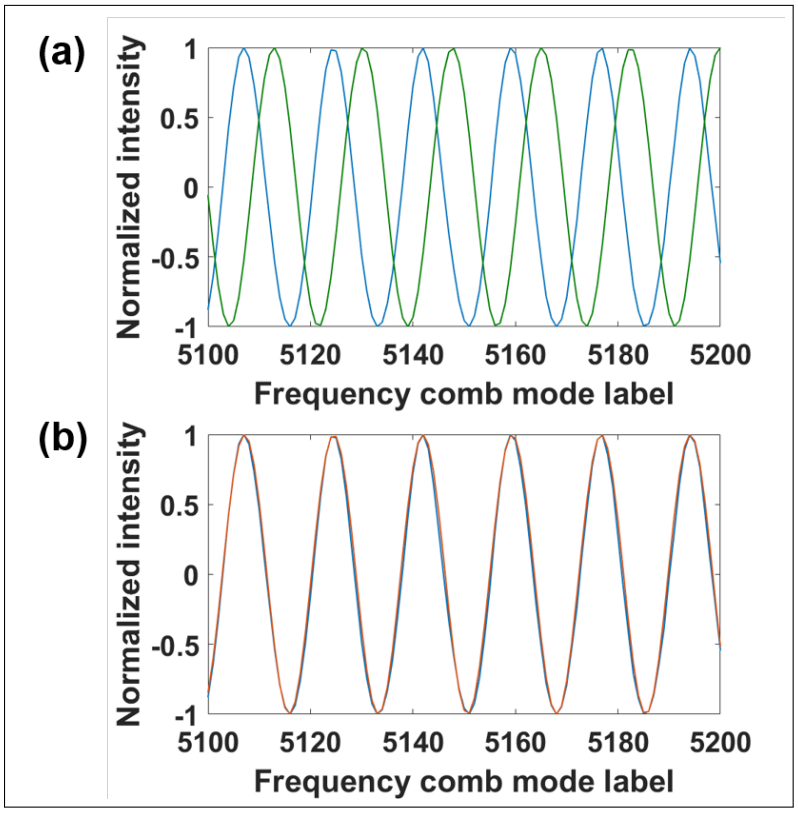

Figure 3.4: Normalized interference intensities and the corrected results. (a) The blue curve shows the normalized result based on Hilbert transform. The green curve is the calculated intensities based on the distance obtained from spectral interferometry method and refractive index of each mode. (b) The blue curve is still the normalized intensities. The red curve is the calculated intensities based on the optimized distance obtained from dispersion correction method and refractive index of each mode.

Fig. 3.5. Therefore, the fitting error is canceled successfully. The results in Fig. 3.6 show

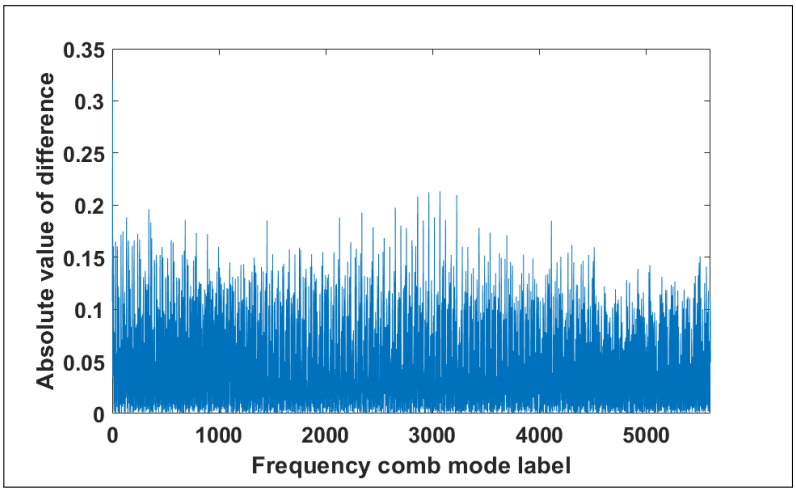

Figure 3.5: Absolute value of difference between the normalized intensity and the optimized result

the differences between the measurements of dispersion correction method and results recorded by HeNe counting interferometry. For each individual measurement the agreement between the frequency comb and the HeNe laser is within 800 nm. After averaged over five measurements,the largest difference is 430 nm. The standard deviation is on average 190 nm. But when we focus on the result for the distance of 5 mm, the agreement decreases to 60 nm and the standard deviation decreases to 40 nm. When the distance is less than 20 m , the result is much better. The comparison measurement shows that homodyne many-wavelength is an accurate method for distance measurement, especially for short distances. Because the observed differences are mainly caused by environmental effects, such as turbulence and vibrations, which is increased for a long distance.

There are several contributions to the measurement uncertainty, the uncertainty of phase measurements, the uncertainty of the HeNe laser and the uncertainty of refractive index of air. The uncertainty of the measured intensities is estimated to 3×10^{-8}. The uncertainty of the HeNe laser which comes from the wavelength uncertainty and the fringe-counting system is estimated to 3×10^{-9}. The standard uncertainty of the refractive index arising from Edlén Equation is estimated to be 10^{-9}. The results obtained with the comb are compared with the HeNe laser, only the difference between two wavelengths are considered. There is another contribution to the measurement uncertainty needed to be considered, which results from vibrations of the carriage on the measurement bench. The data acquisition time for the frequency comb is 10 ms, and for the HeNe it is 100 ms. Since the comb and HeNe measurements are not perfectly synchronized, there are a small distance vibration between these two measurements. This can be estimated by the standard deviation of HeNe measurements, which is 220 nm. When combining the uncertainty contributions mentioned above as a quadratic sum, a total uncertainty of 222 nm for a distance of 50 m is found. For a coverage factor k = 2, corresponding to a 95 coverage interval, the uncertainty equals to 444 nm, which is better

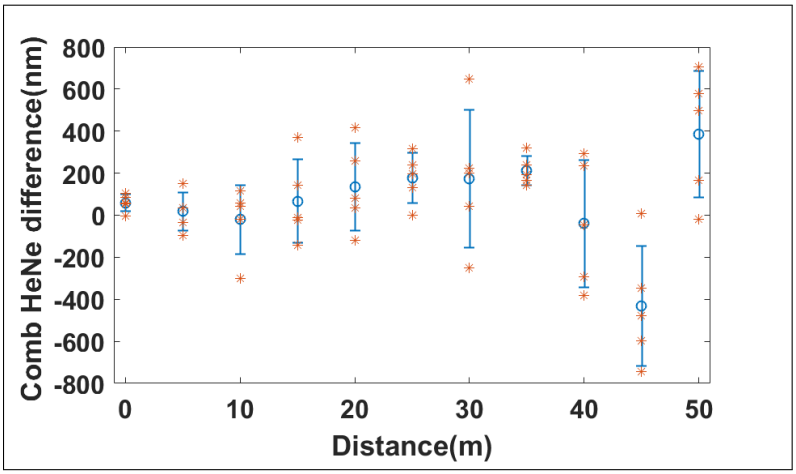

Figure 3.6: The differences between distance measurements with a frequency comb laser and a HeNe laser interferometry for distances up to 50 m. The error bars show the standard deviation of the measurements.

than the uncertainty shown in [12] .

To clearly show the performance of the dispersion correction method clearly, the comparison between the spectral interferometry method and the dispersion correction method is shown in Fig. 3.7. To make the figure clear, the result of individual measurements are not shown. It is clear to see that when distances are less than 20 m, the differences after five measurements are much closer to zero. However for long distances the results of dispersion correction method do not show better performance, sometimes it can be even worse. For instance when we are focusing on the results of 30 m, 45 m and 50m, the error bar after correction is larger. This is mainly because that when using this method, the measurement accuracy of spectral interferometry must be better than $\frac{1}{4}\lambda$. This is easily satisfied when measuring a short distance. For a long distance measurement, the group refractive index dispersion increases. It is also difficult to measure the vibration of refractive index for a long distance. When the accuracy is worse than $\frac{1}{4}\lambda$, the optimized distance with Eq. 3.8 will be wrong. This can make the results worse than previous measurements. This can be easily improved with a longer wavelength frequency comb which can make the $\frac{1}{4}\lambda$ limitation larger, such as 1550 nm. Larger wavelengths has no effect on measurement accuracy, since the accuracy of the spectrally resolved method is independent of the wavelength of the comb.

3.4. CONCLUSION

In this chapter, we have combined the technique of spectral interferometry with dispersion correction for the group refractive index. The measurement done without moving the target can achieve an accuracy within the laser wavelength. Mode resolved interferometry offers the opportunity for this due to the availability of thousands of laser modes for the distance measurement. At present the method shows an agreement within 500 nm with a conventional He-Ne fringe counting interferometer. Further improving

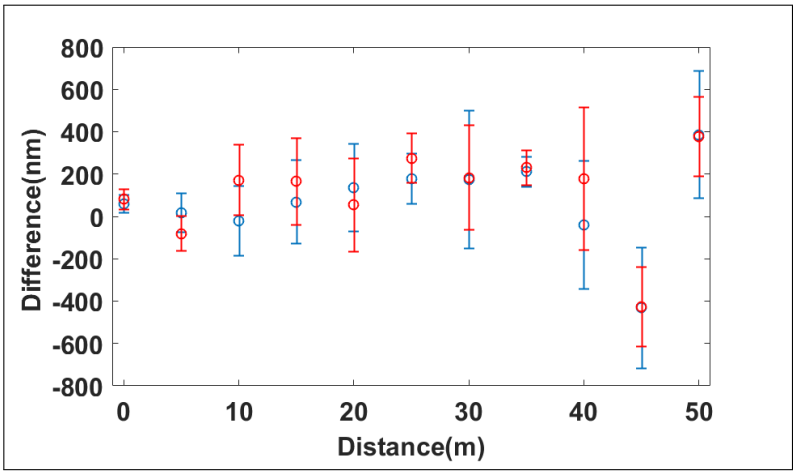

Figure 3.7: The differences between spectral interferometry method and dispersion correction method for distances up to 50 m. The error bars show the standard deviation of the measurements. The blue error bar shows the result of dispersion correction method and the red one shows the result of spectral interferometry method.

the determination of the intensities of the modes will increase the accuracy of this method.

REFERENCES

[1] R. Holzwarth, T. Udem, T. W. Hänsch, J. Knight, W. Wadsworth, and P. S. J. Russell, *Optical frequency synthesizer for precision spectroscopy,* Physical review letters **85**, 2264 (2000).

[2] D. J. Jones, S. A. Diddams, J. K. Ranka, A. Stentz, R. S. Windeler, J. L. Hall, and S. T. Cundiff, *Carrier-envelope phase control of femtosecond mode-locked lasers and direct optical frequency synthesis,* Science **288**, 635 (2000).

[3] N. R. Newbury, *Searching for applications with a fine-tooth comb,* Nature Photonics **5**, 186 (2011).

[4] Y. Salvadé, N. Schuhler, S. Lévêque, and S. Le Floch, *High-accuracy absolute distance measurement using frequency comb referenced multiwavelength source,* Applied Optics **47**, 2715 (2008).

[5] G. Wang, Y.-S. Jang, S. Hyun, B. J. Chun, H. J. Kang, S. Yan, S.-W. Kim, and Y.-J. Kim, *Absolute positioning by multi-wavelength interferometry referenced to the frequency comb of a femtosecond laser,* Optics Express **23**, 9121 (2015).

[6] K. Minoshima and H. Matsumoto, *High-accuracy measurement of 240-m distance in an optical tunnel by use of a compact femtosecond laser,* Applied Optics **39**, 5512 (2000).

[7] J. Ye, *Absolute measurement of a long, arbitrary distance to less than an optical fringe,* Opt. Letters **29**, 1153 (2004).

[8] M. Cui, M. G. Zeitouny, N. Bhattacharya, S. A. van den Berg, H. P. Urbach, and J. J. M. Braat, *High-accuracy long-distance measurements in air with a frequency comb laser,* Opt. Letters **34**, 1982 (2009).

[9] K.-N. Joo, Y. Kim, and S.-W. Kim, *Distance measurements by combined method based on a femtosecond pulse laser,* Opt. Express **16**, 19799 (2008).

[10] M. Cui, M. G. Zeitouny, N. Bhattacharya, S. A. van den Berg, and H. P. Urbach, *Long distance measurement with femtosecond pulses using a dispersive interferometer,* Opt. Express **19**, 6549 (2011).

[11] S. A. van den Berg, S. T. Persijn, G. J. P. Kok, M. G. Zeitouny, and N. Bhattacharya, *Many-wavelength interferometry with thousands of lasers for absolute distance measurement,* Physical Review Letters **108** (2012), 10.1103/physrevlett.108.183901.

[12] S. A. van den Berg, S. van Eldik, and N. Bhattacharya, *Mode-resolved frequency comb interferometry for high-accuracy long distance measurement,* Scientific Reports **5**, 14661 (2015), article.

[13] J. Lee, Y.-J. Kim, K. Lee, S. Lee, and S.-W. Kim, *Time-of-flight measurement with femtosecond light pulses,* Nature Photonics **4**, 716 (2010).

[14] I. Coddington, W. C. Swann, L. Nenadovic, and N. R. Newbury, *Rapid and precise absolute distance measurements at long range,* Nature Photonics **3**, 351 (2009).

[15] T.-A. Liu, N. Newbury, and I. Coddington, *Sub-micron absolute distance measurements in sub-millisecond times with dual free-running femtosecond er fiber-lasers,* Opt. Express **19**, 18501 (2011).

[16] J. Lee, S. Han, K. Lee, E. Bae, S. Kim, S. Lee, S.-W. Kim, and Y.-J. Kim, *Absolute distance measurement by dual-comb interferometry with adjustable synthetic wavelength,* Measurement Science and Technology **24**, 045201 (2013).

[17] M. Shirasaki, *Large angular dispersion by a virtually imaged phased array and its application to a wavelength demultiplexer,* Optics letters **21**, 366 (1996).

[18] S. Xiao and A. Weiner, *2-d wavelength demultiplexer with potential for ≥ 1000 channels in the c-band,* Opt. Express **12**, 2895 (2004), vIPA.

[19] K. G. Larkin, *Efficient nonlinear algorithm for envelope detection in white light interferometry,* JOSA A **13**, 832 (1996).

[20] K. Birch and M. Downs, *An updated Edlén equation for the refractive index of air,* Metrologia **30**, 155 (1993).

4

DISTANCE METROLOGY WITH INTEGRATED MODE-LOCKED RING LASER

The measurement of distance plays an integral part in many aspects of modern societies. In this chapter an integrated mode-locked laser on a chip is used for distance measurement based on mode-resolved interferometry. The emission from the on-chip source with a repetition rate of 2.5 GHz and a spectral bandwidth of 3 nm is coupled into a Michelson interferometer. The interferometer output is recorded as a spectral interferogram, which is captured in a single camera image. The images are analyzed using Hilbert transform to extract the distance. The distance derived shows a deviation of 6 µm from the reference, for a distance up to 25 mm. We also demonstrate interferometry with repetition frequency sweep which can also be used with the source. Performance is expected to be better in the near future with the rapid developments in the field of on-chip laser sources which are demonstrating larger spectral widths and coherence lengths.

4.1. INTRODUCTION

Dimensional metrology has found applications in many areas of modern life. Applications ranging from geodetic monitoring, environmental monitoring and formation flight for interferometry in space to precision engineering require measurements of length or displacement. Laser based interferometric techniques are advancing rapidly due to the new laser sources, advances in detector technology, electronics and computational devices. Pulsed laser sources, which are extremely stable, like the frequency comb, have also led to techniques, which measure larger distances with extremely high accuracies[2–4]. In most cases the experiments that demonstrate these techniques consist of large setups on experimental tables. Applications require devices which can implement dimensional metrology but have a small footprint in terms of size, power consumption

Parts of this chapter have been published in IEEE Photonics Journal **11** No.6 (2019) [1]

and lower cost. These devices could then be used universally to control processes in industry, remote environmental monitoring or flown in satellites.

The development of mode-locked laser sources has been the main instigator of the major leaps made in the field of distance metrology [2]. Significant improvements have been made towards stabilizing mode-locked lasers to an unprecedented level, leading to frequency comb lasers [5]. Optical frequency combs with their extreme stability have found a multitude of applications since their emergence at the beginning of this century [6]. While the goal of the initial applications was to provide an optical frequency standard, the versatility and reliability of frequency combs sparked new research in high-resolution optical spectroscopy and length metrology [7]. Distance metrology has been implemented using methods where the frequency comb is used to reference continuous wave lasers [8–11], as a source for time-of-flight measurement [12] and for the multiplication effect by tuning the repetition frequency f_{rep} [13]. Other applications in spectroscopy and length metrology make use of the strict definition of the optical spectrum, which is directly related to a frequency standard, to extract distance and spectral information from the interferogram of the many individual comb modes. Several techniques based on this method have been successfully demonstrated for distance measurement. These include inter-pulse cross correlation interferometry [14–16], dispersive interferometry [17, 18],spectral interferometry [3, 19] and dual comb multi-heterodyne interferometry [4, 20, 21] which directly use the spectral properties of the frequency comb to extract the distance being measured. Spectral interferometry method is one of the most accurate methods, of which the relative accuracies remain in the $10^{-7} - 10^{-8}$ range mainly due to the uncertainty of the refractive index and are not limited by the performance of the frequency comb.

For the technology to become more accessible for industrial and outdoor measurements, integrating the laser source [22] is desirable. The Ti:Sapphire oscillator based frequency combs are extremely accurate but not so practical for measurements where portable setups or compact devices are required. Fiber-based frequency comb laser sources are portable though the long optical path length in the oscillator results in very low repetition rate, in the order of hundreds of MHz. Since the repetition rate corresponds to the comb mode spacing in the frequency domain, a higher repetition rate, in the order of GHz, loosens the resolution requirements of the spectrometer for spectrometer based measurements. External cavities can be employed to filter some of the comb modes until individual modes can be resolved, but increase the complexity of the system and are sensitive to vibrations [23]. An integrated mode-locked laser on a chip with a high repetition rate can be the key device which can move this technology from laboratories to industrial and outdoor applications. Ideally this device should have a small footprint in size and power consumption. Additionally this device should be sufficiently isolated so that it remains stable in spite of variations in its ambient environment.

In this work we present a distance measurement based on mode-resolved interferometry [19] with a monolithically integrated mode-locked laser [24]. This laser features a repetition rate of 2.5 GHz, which ensures that the modes can be separated by most VIPA (Virtually Imaged Phased Array) spectrometers. Compared to other spectral interferometry methods [19, 25], the phase calculation method with Hilbert transform can extract phase directly and accurately, which can improve fitting results. The performance of

distance measurement and repetition frequency tuning are also shown.

4.2. MEASUREMENT PRINCIPLES

The measurement method is based on a Michelson interferometry. As an input the light from a mode-locked chip laser is used, containing about 120 modes. The laser beam is split into two arms, a reference arm and a measurement arm, and recombined again. Then the combined beam is spectrally resolved by a VIPA spectrometer. The intensity of each mode changes periodically with wavelength. The interference intensity can be written as:

$$I(\phi) = I_0 \cos\phi, \quad \phi = \frac{4\pi L n}{\lambda} \tag{4.1}$$

with I_0 the intensity of the light sent into the interferometer, L, the path length difference of the interferometer arms (single path), λ the vacuum wavelength and. The phase can be written as :

$$\phi = \frac{4\pi L f n}{c}, \tag{4.2}$$

with f the optical frequency and c the speed of light in vacuum. The derivative of phase with respect to frequency can be written as:

$$\frac{d\phi}{df} = \frac{4\pi L}{c}(n + f\frac{dn}{df}) = \frac{4\pi L}{c} n_g, \tag{4.3}$$

with n_g the group refractive index:

$$n_g = n - \lambda \frac{dn}{d\lambda} = n + f\frac{dn}{df}. \tag{4.4}$$

The distance can be written as:

$$L = \frac{d\phi}{df}\frac{c}{4\pi n_g}. \tag{4.5}$$

We define L_{pp} as the pulse-to-pulse distance in the medium, which is written as:

$$L_{pp} = \frac{c}{f_{rep} n_g}, \tag{4.6}$$

with f_{rep} is the repetition frequency of frequency comb. The phase of each mode is obtained by Hilbert transform. If the distance is less than $\frac{1}{4}L_{pp}$, there is no ambiguity to unwrap the phase. Then linear fit is used to obtain the the phase change with frequency. The linear fit result is $\phi = C \cdot p + b$. This implies that the refractive index changes linearly with wavelength. Here C and b are fitting parameters and p is a label which is relative to a specific mode as defined by $f_p = f_{rep}(Q + p) + f_0$, where Q is a very large integer. With $d\phi/df = C/f_{rep}$, this leads to

$$L = \frac{C}{f_{rep}}\frac{c}{4\pi n_g}. \tag{4.7}$$

If the distance being measured is between $\frac{1}{4}L_{pp}$ and $\frac{1}{2}L_{pp}$, C is negative and L can be written as:

$$L = \frac{2\pi + C}{f_{rep}}\frac{c}{4\pi n_g}. \tag{4.8}$$

Just a linear fit is not enough to determine C, because the sign of C is unknown. It is possible to determine C with several methods, such as changing the f_{rep}, which will be shown in the following section.

Within $\frac{1}{2}L_{pp}$ the distance L is defined with non-ambiguity. When L is larger than $\frac{1}{2}L_{pp}$, the interference patterns are repeating for each $\frac{1}{2}L_{pp}$, because the phase change is more than 2π if $L > \frac{1}{2}L_{pp}$. Using the linear fit, we can only obtain phase change which is less than 2π. The arbitrary distance can be written as:

$$L_t = \frac{1}{2}mL_{pp} + L, \tag{4.9}$$

where m is an integer and can also be determined by sweeping the f_{rep}.

4

4.3. EXPERIMENTAL SETUP

The setup for the experiment presented in this work has three main components: the monolithically integrated mode-locked laser, the Michelson interferometer with reference and measurement arm, and the VIPA spectrometer. Optical single-mode fibers are used to transfer the light between those components. A schematic of the setup is shown in Figure 4.1. The different segments and their control parameters are explained in the following sections.

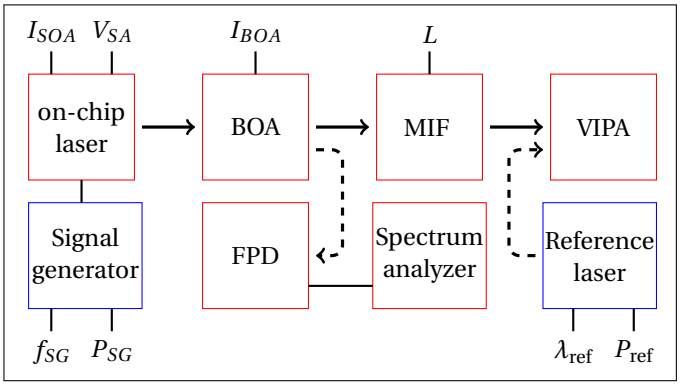

Figure 4.1: The schematic diagram of the experimental setup showing the different parts. Light is collected with a lensed fiber from the on-chip laser and amplified in the booster optical amplifier (BOA). The amplified light is sent to the Michelson interferometer (MIF) with reference and measurement arm. A VIPA spectrometer (VIPA) records interferograms from which the length of the measurement arm can be extracted. A fast photodetector (FPD) in combination with an electronic spectrum analyzer allowed for measuring the repetition rate of the laser. The light is guided with single-mode fibers between the different parts of the setup. A signal generator was used for hybrid mode-locking.

4.3.1. MONOLITHICALLY INTEGRATED LASER

A monolithically integrated mode-locked laser, with a repetition rate of $f_{\text{rep}} \approx 2.5$ GHz at a wavelength of 1.58 µm, was realized on the InP-based multi-project wafer run by SMART Photonics [26]. The laser features a 33 mm long cavity ring. Phase-control el-

ements, gain sections and saturable absorbers in the cavity allow for tuning and optimization of the laser output. The chip was mounted on an aluminum sub-carrier and the electrical contacts wire-bonded to a printed circuit board, which allowed for easier electrical access for controlling the laser. The laser was operated at room temperature without any active cooling or temperature stabilization. The mode-locking of the laser could be achieved either by passive means or by using hybrid mode-locking. Passive mode-locking was realized applying DC (direct current) bias to the saturable absorber and the gain segments. In the case of hybrid mode-locking an additional RF (radio frequency) signal was fed to the absorber via a bias tee, which matched the f_{rep} of the chip in passive mode-locking operation. In hybrid mode-locking f_{rep} could be pinned to a fixed value over the course of the entire experiment, while in a passively locked operation the repetition rate of the laser experienced drift. The current control of the laser was driven by a Thorlabs LDC8005 in a PRO8000 chassis. The saturable absorber was controlled with a National Instruments NI9923 in cDAQ-9178 chassis. The RF signal was provided by a Rohde & Schwarz SMB100A signal generator. The chip featured angled output ports with anti-reflective coatings, from which the light was collected with a tapered fiber (OZ-optics TSMJ-EA-1550-9/125-0.25-7-2.5-14-1-AR). In this experiment the light from the mode-locked laser was amplified through a booster optical amplifier (BOA) S9FC1004P by Thorlabs, which is a semiconductor based amplifier. An APC circulator, Thorlabs 6015-3, was placed before the BOA to prevent light from the BOA from entering the chip and disturbing the laser operation. The repetition frequency of the laser was measured with a fast photo-detector (Newport 818-BB-35F) in combination with a RIGOL DSA1030 spectrum analyzer. For hybrid mode locking the signal generator provided an RF signal with matching frequency $f_{SG} = f_{\text{rep}}$ and an output power of $P_{SG} = 10\,\text{dBm}$. A typical mode-resolved spectrum recorded by VIPA spectrometer has been shown in Figure 4.2. The intensity of each mode is modulated by VIPA and this modulation can be canceled by the normalization. The further details of the pulsed laser on a chip have already been reported by Latkowski [24].

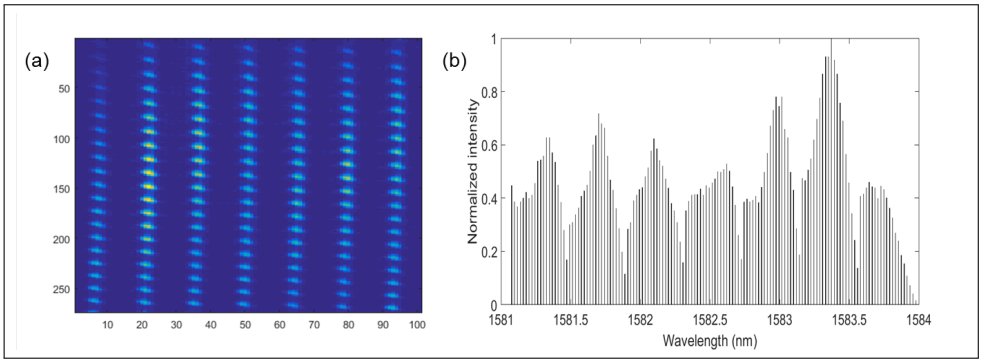

Figure 4.2: (a) The two-dimensional VIPA image as recorded by the camera containing the spectral information. (b)VIPA modulated spectrum obtained from the image shown in (a).

4.3.2. MICHELSON INTERFEROMETER

One of the key components for the distance measurement setup is the Michelson interferometer. The path length difference between the known reference arm and variable measurement arm results in an interferogram on the VIPA spectrometer. For the short distance measurement, the measurement arm was varied using the translation stage M-112.1DG from PI with a total movement range of 25 mm. A PI C-863 DC motion controller was used to drive the translation stage. For the long distance measurement, the measurement arm has a maximum length of 1.5 m and consists of a long rail with electric carriage.

4.3.3. VIPA SPECTROMETER

The virtually imaged phased array spectrometer consists of several components, which are shown in Figure 4.3. In the spectrometer the combination of cylindrical lens and VIPA etalon results in wavelength-dependent transmission for different angles and thus acts as an angular disperser. The VIPA etalon from Precision Photonics (S-LAA71) consists of a 1.75 mm thick glass plate. The front side of the etalon is covered with a highly reflective coating with a reflectance of 99.5%, except of a small window, which is left uncoated to allow the beam to enter the etalon. The output side's coating provided a reflectance of 96%. A small angle between the etalon and the incoming beam allows for several reflections within the etalon. The transmission can be explained with the creation of an array of virtual light sources, which can constructively interfere if angle and wavelength are matched [27, 28], thus causing angular dispersion in the vertical plane. The VIPA etalon has a high resolution, but a low free spectral range (FSR), so the spectral orders overlap, therefore a grating, Spectrogon UK (G1100 31x50x10 NIR, 1100 lines/mm), in orthogonal orientation is used as a post-disperser, creating dispersion in the horizontal plane. The angularly dispersed beam is then focused onto different positions on the detector plane of the camera, by a lens, where each position corresponds to an optical frequency. A continuous broadband light source would create a vertical line pattern on the infrared camera, XenICs (XEVA-FPA-1.7-640). If the spectrometer allows for a separation of the individual laser modes, a point pattern will be visible, as shown in references[3, 23]. The spectral data is extracted by relating the position on the camera plane to its corresponding frequency. This is done by following the lines or the lines of dots on the camera image. When following one line, spectral data for the span of one FSR of the VIPA can be obtained. To exceed this wavelength range, neighboring lines have to be read out in the same fashion, which allows for stitching of the complete spectra out of the contributions of the individual lines of the camera image[3, 23]. In this experiment the VIPA spectrometer had a resolution of 680 MHz with an FSR of 50 GHz for a single line. The modes of the laser, which are spaced by 2.5 GHz, are spectrally resolved by the VIPA spectrometer. The VIPA spectrometer was calibrated with an Agilent 6015-3-APC tunable single-mode laser in an 8163B mainframe, which allowed for identifying the FSR and also provided the wavelength calibration. This calibration is only used to get the correct stitching of the spectra.

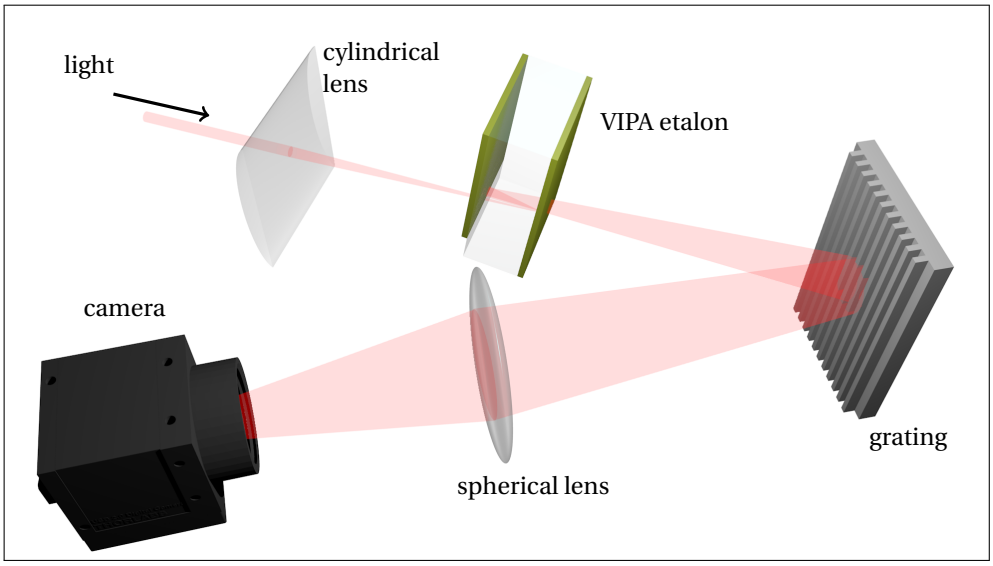

Figure 4.3: A schematic of the VIPA spectrometer. Light is focused using a cylindrical lens on the VIPA etalon which then disperses the light spectrally in the y-direction. A grating is used as a post-disperser in the x-direction to separate the different orders. The angularly dispersed frequency information is then converted to position information on a camera.

4.4. RESULTS AND DISCUSSION

In order to test the ability of distance measurement with the integrated mode-locked ring laser, we measured a short distance using a high accuracy translation stage and a long distance which were measured simultaneously with the laser and counting HeNe interferometer for comparison. We also swept the repetition frequency to see the change in the fringes. The results will be shown in the following sections.

4.4.1. REPETITION FREQUENCY SWEEP FOR DETERMINATION OF C

The technique used to extract the distance reported in this chapter requires knowledge of the sign of fitting parameter C. One method to solve this problem is to change the f_{rep}. When the laser is hybrid mode locked, f_{rep} is much easier to change. Figure 4.4 shows the fitting results with different repetition frequency. The relation between C and f_{rep} is almost linear and allows the determination of the sign of C. This is especially significant for absolute distance measurement for a long distance. From the particular example Figure 4.4, it is found that C is positive.

4.4.2. DISTANCE MEASUREMENT FOR SHORT DISTANCE

The distance measurements were performed with a high accuracy translation stage which has a unidirectional repeatability of 0.1 µm. Initially the carriage was positioned at the beginning of the stage and the images of the initial position were recorded. Then the carriage was moved in 5 mm increments, and images were taken. At every position, five

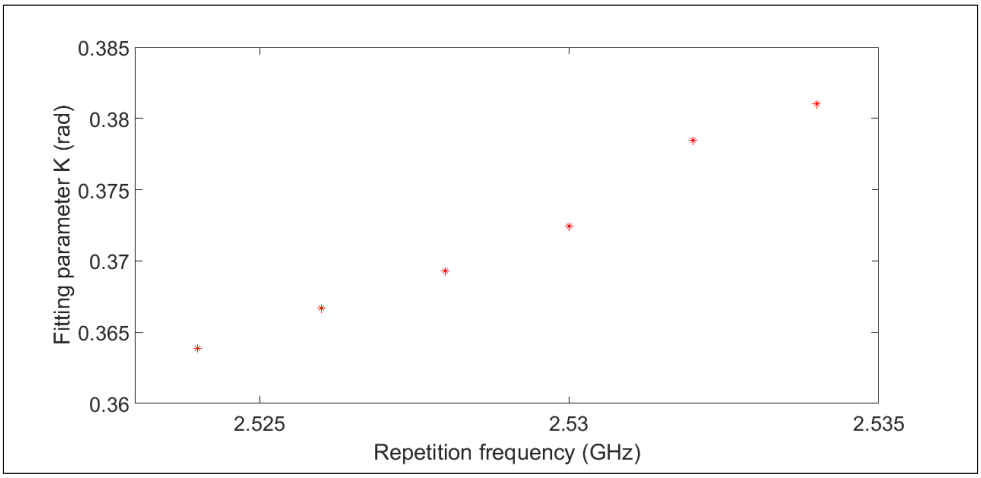

Figure 4.4: The fitting results for different repetition frequency. The repetition frequency is changed from 2.524 to 2.534 GHz in 2 MHz increments

measurements were recorded. The environment conditions were well controlled in the clean room. A typical phase measurement and unwrapped phase with a linear fit are shown in Figure 4.5. Each sample on the horizontal axis corresponds to a wavelength of the frequency comb.

The optical distance measurement is compared with the value given by the translation stage. Figure 4.6 shows the outcome of this analysis. When averaged over five measurements the integrated comb laser and the length given by the translation stage agree within 6 µm with a standard deviation of 1.4 µm.

The linear fitting uncertainty is less than 5×10^{-4}, which corresponds to $12.5 \mu m$. This is the main contribution to the distance measurement uncertainty, which is much larger than the group refractive index and environmental effects. This error is mostly arising from the limited number of modes available from the laser. Several simple improvements will enhance the accuracy of a device based on this experiment. For the chip used in this work the spectral bandwidth is 3 nm (120 modes) in comparison to the measurement with several thousands of modes reported by Van den Berg [19] using a Ti:Sapphire laser. New mode-locked laser designs already extend the bandwidth to 40 nm [24, 29], so this will not be a bottleneck in taking the technology further. Another easy improvement can be increasing the repetition frequency. As shown in [25], with a laser of tens of gigahertz repetition frequency a highly accurate result can be also obtained.

4.4.3. DISTANCE MEASUREMENT FOR LONG DISTANCE

A distance up to 70 cm was also measured with chip laser. The setup is similar to short distance measurement, except a 1.5 m bench was used to replace the translation stage. The displacement of the bench could not be directly read out, therefore a counting HeNe interferometer was used for comparison. However, the results of long distance measurements were much worse than short distance measurement. The integrated comb laser

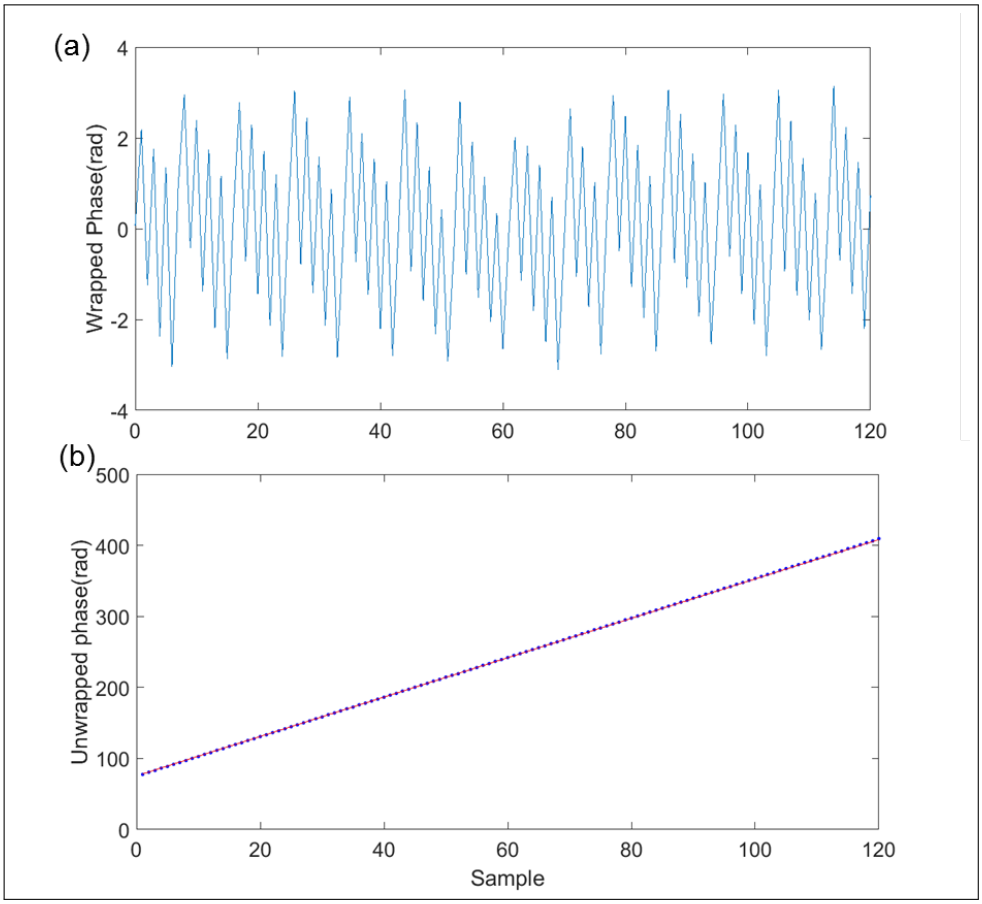

Figure 4.5: Typical phase measurements and fitting result. (a) The wrapped phase obtained by Hilbert transform for 120 modes. (b) The unwrapped phase - blue points and linear fit - red line.

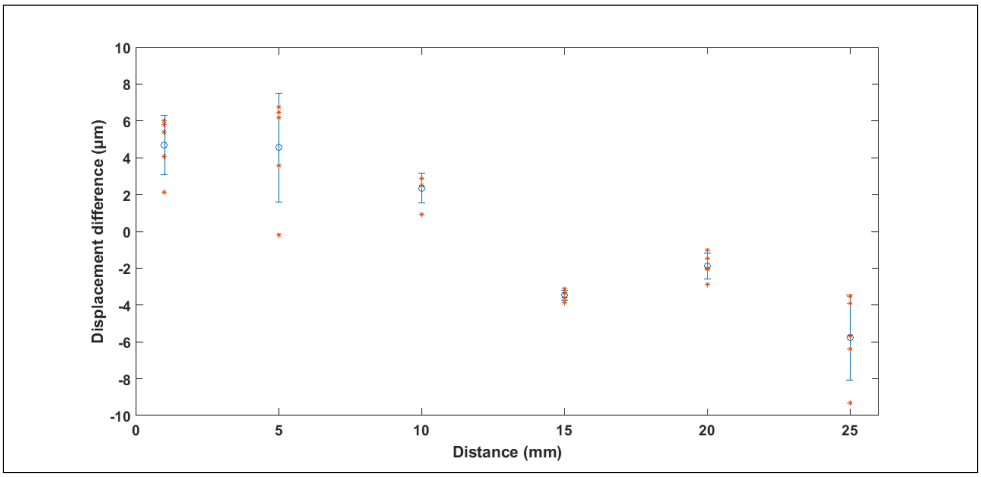

Figure 4.6: The displacement differences between distance measurements with a integrated comb laser and length given by the translation stage for distances up to 25 mm. The error bars show the standard deviation of the measurements.

and counting HeNe interferometer measurements agree within 5 mm over a distance of 70 cm. Though as mentioned in [19], the method does not need the offset frequency f_0 to be locked, it only works when the distance is less than $\frac{1}{2}L_{pp}$. If the distance is longer than $\frac{1}{2}L_{pp}$, the interference occurs between different pulses. The interference signal changing with distance is shown in Figure 4.7. The interference fringes at the distance of 0.7 cm can be clearly seen but for a distance of 70 cm the fringes almost disappear. The pulses at different moment are not stable in frequency and the interference is not stable enough to be recorded. The interference signal is not DC anymore. The integration time of camera is 10 ms, which means that the image is obtained by averaging 2.5×10^7 pulses. The averaging reduces the interference signal and increases the uncertainty of fitting result. A new laser has been published with a 12-nm 10-dB output optical spectrum and a narrow longitudinal mode linewidth (<400 kHz)[30]. This new laser can dramatically improve the measurement range at these distances.

4.5. CONCLUSION

We have shown that mode-resolved spectral interferometry with an on-chip laser is possible. This is promising for frequency comb-based distance measurement, since miniaturization allows for potentially huge cost reduction, reduction of energy consumption and footprint, which could enable a wide range of applications for which current frequency comb systems are too bulky and expensive. A tunable mode-locked laser can easily solve the ambiguity problem of spectral interferometry method by varying the repetition frequency, which is significant for absolute long distance measurement. However, further improvement on spectral width and coherence length will be needed to reach the results obtained with traditional frequency comb sources. Given the rapid developments in the field, though, competing performance may be demonstrated in

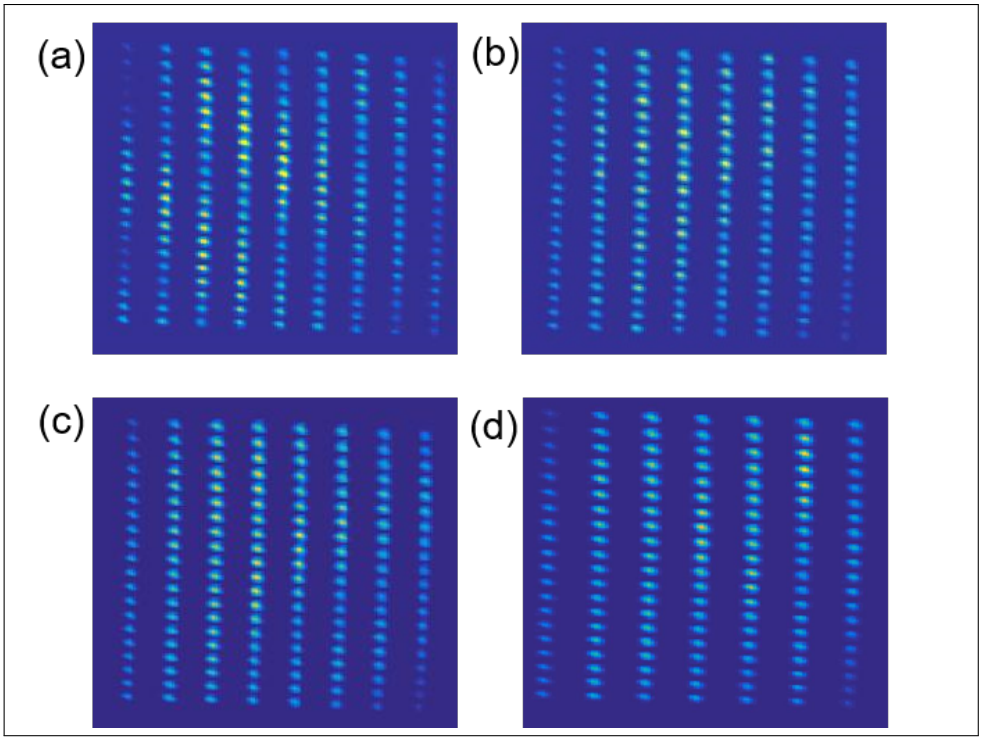

Figure 4.7: VIPA images of the interference for different displacements. The arm length differences for the images are (a) $L = 0.7\,\text{cm}$, (b) $L = 19\,\text{cm}$, (c) $L = 40\,\text{cm}$, and (d) $L = 70\,\text{cm}$.

near future. Several improvements of lasers like larger bandwidth [24, 29] and narrow linewidth [30] have been reported, which will further enhance the stability of the on-chip laser and improve the measurement accuracy for a wide range of applications.

REFERENCES

[1] K. Hei, G. Shi, A. Hänsel, Z. Deng, S. Latkowski, S. A. Van den Berg, E. Bente, and N. Bhattacharya, *Distance metrology with integrated mode-locked ring laser,* IEEE Photonics Journal **11**, 1 (2019).

[2] K. Minoshima and H. Matsumoto, *High-accuracy measurement of 240-m distance in an optical tunnel by use of a compact femtosecond laser,* Appl. Opt. **39**, 5512 (2000).

[3] S. A. van den Berg, S. T. Persijn, G. J. P. Kok, M. G. Zeitouny, and N. Bhattacharya, *Many-wavelength interferometry with thousands of lasers for absolute distance measurement,* Physical Review Letters **108** (2012), 10.1103/physrevlett.108.183901.

[4] I. Coddington, W. C. Swann, L. Nenadovic, and N. R. Newbury, *Rapid and precise absolute distance measurements at long range,* Nature Photonics **3**, 351 (2009).

[5] J. L. Hall, *Optical frequency measurement: 40 years of technology revolutions,* IEEE Journal of Selected Topics in Quantum Electronics **6**, 1136 (2000).

[6] S. A. Diddams, *The evolving optical frequency comb [invited],* J. Opt. Soc. Am. B **27**, B51 (2010).

[7] N. R. Newbury, *Searching for applications with a fine-tooth comb,* Nature Photonics **5**, 186 (2011).

[8] T. Yoon, J. Ye, J. Hall, and J.-M. Chartier, *Absolute frequency measurement of the iodine-stabilized he-ne laser at 633 nm,* Appl. Phys. B **72**, 221 (2001).

[9] Y. Salvadé, N. Schuhler, S. Lévêque, and S. Le Floch, *High-accuracy absolute distance measurement using frequency comb referenced multiwavelength source,* Applied Optics **47**, 2715 (2008).

[10] S. Hyun, M. Choi, B. J. Chun, S. Kim, S.-W. Kim, and Y.-J. Kim, *Frequency-comb-referenced multi-wavelength profilometry for largely stepped surfaces,* Optics Express **21**, 9780 (2013).

[11] E. Baumann, F. R. Giorgetta, J.-D. Deschênes, W. C. Swann, I. Coddington, and N. R. Newbury, *Comb-calibrated laser ranging for three-dimensional surface profiling with micrometer-level precision at a distance,* Optics Express **22**, 24914 (2014).

[12] J. Lee, Y.-J. Kim, K. Lee, S. Lee, and S.-W. Kim, *Time-of-flight measurement with femtosecond light pulses,* Nature photonics **4**, 716 (2010).

[13] Y. Nakajima and K. Minoshima, *Highly stabilized optical frequency comb interferometer with a 9 long fiber-based reference path towards arbitrary distance measurement,* Opt. Express **23**, 25979 (2015).

[14] J. Ye, *Absolute measurement of a long, arbitrary distance to less than an optical fringe,* Opt. Letters **29**, 1153 (2004).

[15] M. Cui, M. G. Zeitouny, N. Bhattacharya, S. A. van den Berg, H. P. Urbach, and J. J. M. Braat, *High-accuracy long-distance measurements in air with a frequency comb laser,* Opt. Letters **34**, 1982 (2009).

[16] P. Balling, P. Křen, P. Mašika, and S. van den Berg, *Femtosecond frequency comb based distance measurement in air,* Opt. Express **17**, 9300 (2009).

[17] K.-N. Joo, Y. Kim, and S.-W. Kim, *Distance measurements by combined method based on a femtosecond pulse laser,* Opt. Express **16**, 19799 (2008).

[18] M. Cui, M. G. Zeitouny, N. Bhattacharya, S. A. van den Berg, and H. P. Urbach, *Long distance measurement with femtosecond pulses using a dispersive interferometer,* Opt. Express **19**, 6549 (2011).

[19] S. A. van den Berg, S. van Eldik, and N. Bhattacharya, *Mode-resolved frequency comb interferometry for high-accuracy long distance measurement,* Scientific Reports **5**, 14661 (2015), article.

[20] T.-A. Liu, N. Newbury, and I. Coddington, *Sub-micron absolute distance measurements in sub-millisecond times with dual free-running femtosecond er fiber-lasers,* Opt. Express **19**, 18501 (2011).

[21] R. Yang, F. Pollinger, K. Meiners-Hagen, M. Krystek, J. Tan, and H. Bosse, *Absolute distance measurement by dual-comb interferometry with multi-channel digital lock-in phase detection,* Measurement Science and Technology **26**, 084001 (2015).

[22] L. C. Sinclair, I. Coddington, W. C. Swann, G. B. Rieker, A. Hati, K. Iwakuni, and N. R. Newbury, *Operation of an optically coherent frequency comb outside the metrology lab,* Opt. Express **22**, 6996 (2014).

[23] R. Šmíd, A. Hänsel, L. Pravdová, J. Sobota, O. Číp, and N. Bhattacharya, *Comb mode filtering silver mirror cavity for spectroscopic distance measurement,* Review of Scientific Instruments **87**, 093107 (2016), http://dx.doi.org/10.1063/1.4962681.

[24] S. Latkowski, V. Moskalenko, S. Tahvili, L. Augustin, M. Smit, K. Williams, and E. Bente, *Monolithically integrated 2.5 ghz extended cavity mode-locked ring laser with intracavity phase modulators,* Opt. Lett. **40**, 77 (2015).

[25] A. Lešundák, D. Voigt, O. Cip, and S. van den Berg, *High-accuracy long distance measurements with a mode-filtered frequency comb,* Opt. Express **25**, 32570 (2017).

[26] SMART Photonics B.V. ; http://www.smartphotonics.nl, .

[27] A. Vega, A. M. Weiner, and C. Lin, *Generalized grating equation for virtually-imaged phased-array spectral dispersers,* Appl. Opt. **42**, 4152 (2003).

[28] S. Xiao and A. Weiner, *2-d wavelength demultiplexer with potential for ≥ 1000 channels in the c-band,* Opt. Express **12**, 2895 (2004), vIPA.

[29] V. Moskalenko, J. Koelemeij, K. Williams, and E. Bente, *Study of extra wide coherent optical combs generated by a qw-based integrated passively mode-locked ring laser,* Opt. Lett. **42**, 1428 (2017).

[30] Z. Wang, K. van Gasse, V. Moskalenko, S. Latkowski, E. A. J. M. Bente, B. Kuyken, and G. Roelkens, *A iii-v-on-si ultra-dense comb laser,* Light-Sciences and Applications **5**, e16260 (2017).

5

ABSOLUTE DISTANCE MEASUREMENT WITH GAIN-SWITCHED DUAL OPTICAL FREQUENCY COMB

The measurement of distance plays an important role in many aspects of modern societies. In this chapter, an absolute distance measurement method for arbitrary distance is proposed and demonstrated using mode-resolved spectral interferometry with a gain-switched dual comb. An accuracy of 12 µm, when compared to a He-Ne fringe counting laser interferometer, for a displacement up to 2.5 m is demonstrated by tuning the repetition frequency of the dual comb from 1.1 GHz to 1.4 GHz. The compact measurement system based on a gain-switched dual comb breaks the constraint of periodic ambiguity. The simplification and improvements are significant for further industrial applications.

5.1. INTRODUCTION

With the rapid development of science and technology, distance measurement plays an important role in modern life, especially in monitoring tolerances in industrial manufacturing. Time-of-flight method using laser pulses is the most direct way to measure absolute distances. However, the limited electrical bandwidth of the available high-speed photoreceivers restricts the detection resolution, between the optical pulses, to picoseconds (ps). The latter limits the detection resolution to the millimeter range [2]. Laser based interferometric techniques overcome this restriction by measuring the phase difference between the interference light. Among these techniques, the methods based on the optical frequency comb (OFC) are developing rapidly. These methods use a stabilized mode locked laser (MLL) as the OFC source and can measure long distances with

Parts of this chapter have been published in Optics Express **29** No.6 (2021) [1]

extremely high accuracies [3–5]. The frequency comb was firstly applied in distance measurement by Minoshima, where the phase of the intermode beats of the frequency comb were measured to determine the distance [6]. Cross correlation measurements based on inter-pulse interference in a Michelson interferometer came thereafter [7, 8]. In order to satisfy the industrial demands on the measurement precision, dispersive interferometry [9, 10], spectrally resolved interferometry [4, 11], time-of-flight measurement [12] and dual comb interferometry [5, 13, 14] were subsequently proposed and demonstrated .

Distance measurement, based on spectrally resolved interferometry, realized accurate and long distance measurements with a single frequency comb [4, 11]. Here, the frequency comb is used as a multiple wavelength laser source that is fed to the input of a Michelson interferometer. The individual modes superpose after travelling from the two arms. The interference pattern is then spectrally resolved by a virtually imaged phase array (VIPA) spectrometer. The difference in distance between the two arms can be obtained after unravelling the interference pattern and extracting the phase changes. One of the main constraints in using this technique for industrial and outdoor measurements is the complex instrumentation. The VIPA spectrometer needs space, careful alignment and has many components. It is not suitable for low repetition rate combs due to its resolution limitation. Simplification of the instrumentation has been demonstrated by replacing the VIPA with a single grating, while using a Fabry-Pérot (FP) cavity to filter the frequency spectrum of the laser [15]. On the other hand FP cavities add their own complexity. Some other issues that this technique has is that when the distance is an integer multiple of the pulse-to-pulse distance L_{pp}, this method fails to yield a result. At these distances the solution is to tune the repetition frequency of the comb putting higher demands on the laser.

The dual frequency comb spectrometer, having no moving parts and being able to resolve the spectra of the frequency comb is quite promising for immediate applications. The technique uses a pair of OFCs with slight differences in their repetition frequencies. The signals from the two combs interfere on a photodetector and the beat spectra yields an RF comb, which maintains the spectral information encoded in the optical domain. The dual comb technique has gained popularity as it significantly reduces the complexity of the receiver and offers high precision, fast acquisition times and potentially low bandwidth receivers [16]. Typically, OFCs employed in dual comb spectroscopy (DCS) have utilised MLLs. However, the fabrication of these devices is often costly and complex, and due to the physical nature of the devices, they possess a fixed repetition frequency. For tunability of the repetition frequency, electro-optic modulators may be a viable alternative. However, this OFC generation technique requires cascaded [17] or dual drive modulators [18] to generate broad and flat OFCs. Along with this drawback, the technique will inherently suffer from instabilities due to bias drift [19]. To combat this bias drift, a dc bias control feedback may be required to ensure that OFCs remain stable [20].

The dual comb in this chapter is generated by two cost-efficient commercially available lasers, which have been gain switched. The gain switching technique provides a simple and flexible method for the generation of OFCs, which allows for tuning of both the wavelength and the repetition frequencies of the OFCs [21]. Some drawbacks of the

gain switching technique to generate OFCs are overcome by external optical injection locking (OIL) utilizing a maser-slave configuration. The spectral flatness and the number of generated comb tones are both improved. Furthremore, external OIL results in the effective transference of the master laser's narrow linewidth to each of the individual comb lines [22]. This transference of the master laser's narrow linewidth is utilised in the dual comb architecture presented here, where both individual OFCs are injection locked using a single tunable laser (TL). This provides phase and repetition frequency locking, resulting in high phase coherence between the OFCs.

In this chapter, we present a distance measurement based on spectrally resolved interferometry [11] with a gain-switched dual optical comb [23]. This laser features a repetition frequency that can be tuned over 300 MHz, between 1.1 GHz to 1.4 GHz. Based on the broad tuning range of the gain switched dual comb, an absolute distance measurement method for arbitrary distance is reported along with a comparison measurement with a fringe counting helium-neon (HeNe) laser interferometer.

5.2. EXPERIMENTAL SETUP

A schematic of the dual comb source and the absolute distance measurement setup is shown in Fig. 5.1. The dual comb architecture used in this work is shown in Fig. 5.1 on the left side. It comprises two Fabry-Pérot (FP) lasers, acting as slave lasers in a dual master-slave configuration. Utilizing FP lasers allows for tunable dual comb generation across the entire C-band [22]. Both FPs are gain switched [21] using sine waves, amplified to 24 dBm, at frequencies of 1.25 (signal comb) and 1.251 GHz (local oscillator) respectively. The individual OFCs are mutually injection locked, using a single master semiconductor tunable laser (STL), which provides phase synchronization between both slave (FP) lasers. A typical RF beat tone spectra measured using an electrical spectrum analyzer are shown in Fig. 5.2. After the dual comb is generated, the signal comb is sent into a Michelson interferometer, where the laser beam is split into two arms, a reference arm and a measurement arm, and recombined. The interference beam is then combined with the LO comb using a 50/50 coupler and detected using a balanced detector. An RF spectrum analyser is used to resolve the comb and record the interference signal.

One of the key components for the distance measurement setup is the Michelson interferometer. The measurement arm of the Michelson interferometer can be moved over a distance of 2.5 m with a motor driven carriage carrying the retroreflector. In order to verify the distance measurement ability, the reading of the HeNe displacement interferometer and frequency comb measurement are compared for each measurement point.

5.3. MEASUREMENT PRINCIPLES

5.3.1. SPECTRAL INTERFEROMETRY WITH DUAL COMB

Mathematically, the reference comb, measurement comb and the LO comb could be described as below:

$$E_{mea} = \sum_{m} A_m \cos\left[2\pi(m f_{rep,sig} + f_{sig})t - \phi_m\right] \tag{5.1}$$

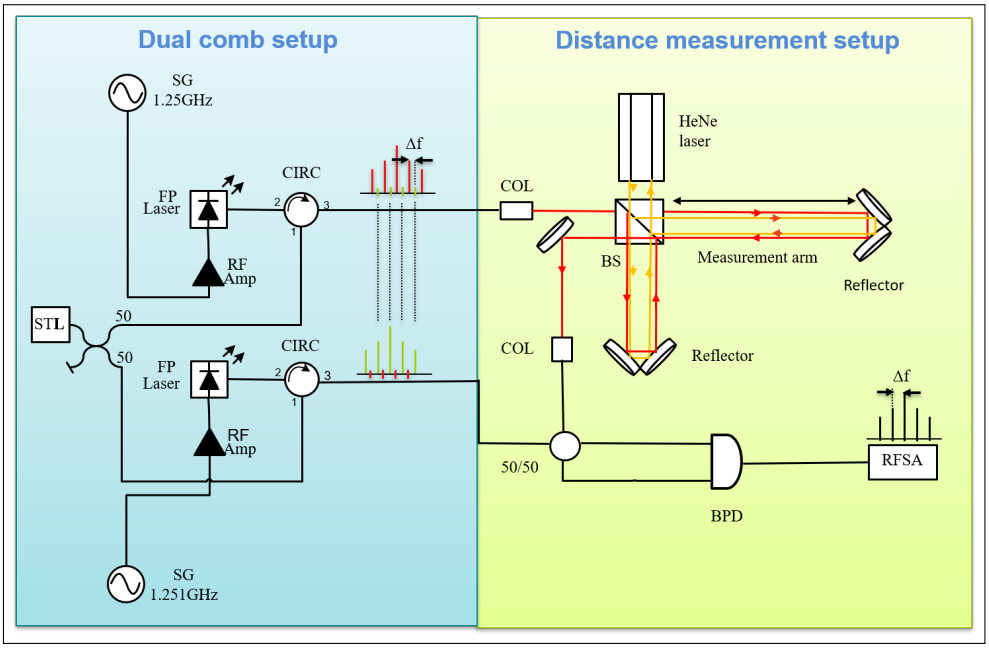

Figure 5.1: Schematic overview of the measurement setup. The dual comb is generated by a semiconductor tunable laser (STL) and two Fabry Pérot (FP) lasers. The FP lasers are gain switched by two RF signals from by two signal generators (SG) and amplified by two RF amplifiers (Amp). The signal comb (red), which is the output of an optical circulator (CIRC), is sent to a Michelson interferometer by optical fibers and a collimator (COL). The signal is sent to a balanced photodetector (BPD) by a 50/50 coupler after being split and recombined by the beam splitter (BS). The LO comb is directly sent to the BPD by optical fibers, a CIRC, and the same 50/50 coupler. The resulting baseband beat signals are recorded by an RF spectrum analyzer (RFSA). Both the HeNe laser (yellow line) and dual comb laser (red line) measure the displacement quasi-simultaneously.

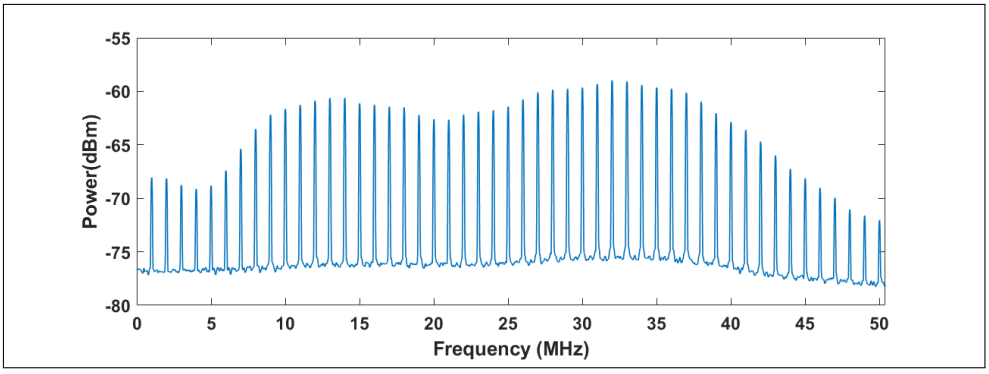

Figure 5.2: RF beat tone spectra measured using an electrical spectrum analyzer.

$$E_{ref} = \sum_m A_m \cos\left[2\pi(m f_{rep,sig} + f_{sig})\, t\right] \tag{5.2}$$

$$E_{LO} = \sum_m B_m \cos\left[2\pi(m f_{rep,LO} + f_{LO})\, t\right] \tag{5.3}$$

where E_{ref} and E_{mea} are the electric fields of the signal pulses reflected from the reference arm and the measurement arm, respectively, $f_{rep,sig}$ and f_{sig} are the repetition frequency and the frequency of the first mode of the comb, respectively. ϕ is the phase difference between the reference arm and the measurement arm. E_{LO} represents the electric field of the local oscillator (LO) pulse, where the repetition rate and the frequency of the first mode of the comb are $f_{rep,LO}$ and f_{LO}. There is a slight difference between $f_{rep,sig}$ and $f_{rep,LO}$, which is represented by Δf_{rep}. The signal pulse and the LO pulse are slaves to the same master oscillator, thus f_{sig} and f_{LO} are equal [23]. Therefore the output intensity is $|(E_{mea} + E_{ref}) + E_{LO}|^2$. The detection is done using a balanced detector so the DC terms of the intensity are canceled, and only the correlative terms $(E_{mea} + E_{ref})E_{LO}$ remain. The output intensity can be written as:

$$I_{out} = \sum_m 2A_m B_m \cos\frac{\phi_m}{2} \cos\left[2\pi(m f_{rep,sig} + f_{sig})\, t - \frac{\phi_m}{2}\right] \cos\left[2\pi(m f_{rep,LO} + f_{LO})\, t\right] \tag{5.4}$$

The limited bandwidth of the detector ensures that the high frequency components are filtered out. The intensity without the high frequency part can be written as:

$$I_{out} = \sum_m I_m = \sum_m A_m B_m \cos\frac{\phi_m}{2} \cos(2\pi m \Delta f_{rep}\, t - \frac{\phi_m}{2}) \tag{5.5}$$

Here I_m is the intensity of the single frequency mode. A spectrum analyzer is used to analyse the output signal. The power of RF signals with different frequencies are extracted separately. The measurement with spectrum analyzer improves the signal to noise ratio and is similar to using lock-in detection [24]. This is in contrast to the fast Fourier transform method [5] which cannot be used here since the repetition frequency needs to be swept continuously in order to realize absolute arbitrary distance measurement and a frequency change during a sampling period would lead to error. Using a spectrum analyzer precludes these errors due to the frequency change. The output voltage can be written as:

$$P_m = \frac{(I_m \Re)^2}{r} = {A_m}^2 {B_m}^2 \Re^2 (\frac{1}{2} - \cos\phi_m). \tag{5.6}$$

Here $\Re$ is the responsivity of the photodiode and r is the RF input impedance of the spectrum analyzer. Once the power spectrum is obtained, the signal of the spectrum is filtered with the FFT filter, which can remove the DC terms [25]. The phase of the respective frequency comb modes can then be extracted by the Hilbert transform[26], and can be written as:

$$\phi_m = \frac{4\pi L(m f_{rep,sig} + f_{sig})n}{c}, \tag{5.7}$$

with L the distance difference between the reference arm and measurement arm. Here c is the speed of light in vacuum and n is the air refractive index. The derivative of phase

with respect to m can be written as:

$$\frac{d\phi}{dm} = \frac{4\pi L f_{rep,sig}}{c}(n + (mf_{rep,sig} + f_{sig})\frac{dn}{d(mf_{rep,sig} + f_{sig})}) = \frac{4\pi L f_{rep,sig}}{c} n_g, \quad (5.8)$$

with n_g the group refractive index. The distance can be written as:

$$L = \frac{d\phi}{dm}\frac{c}{4\pi f_{rep,sig} n_g}. \quad (5.9)$$

After unwrapping the phases of each mode, a simple linear fit of the phases gives the slope $C = \frac{d\phi}{dm}$. Plots of a typical experimental data, at different stages of the data processing procedure described above, is shown in Fig. 5.3.

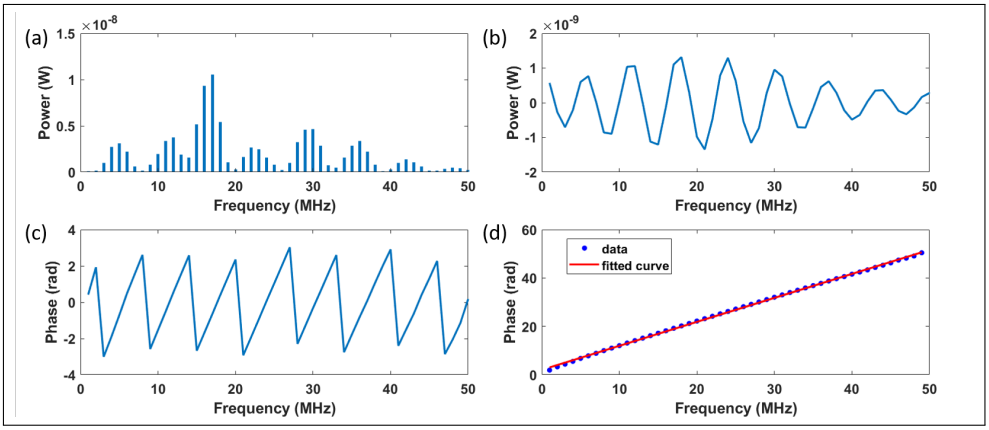

Figure 5.3: Data processing procedure to obtain distance L; (a) typical interference spectrum captured by the RF spectrum analyzer, (b) interference spectrum filtered by FFT and inverse FFT method, (c) the wrapped phase obtained by Hilbert transform and (d) the unwrapped phase (blue points) and linear fit result (red line).

5.3.2. ABSOLUTE DISTANCE MEASUREMENT

We define L_{pp} as the pulse-to-pulse distance in the medium, which is written as:

$$L_{pp} = \frac{c}{f_{rep,sig} n_g}. \quad (5.10)$$

When the measured distance is less than $\frac{1}{4}L_{pp}$, the phase is determined with no ambiguity. If the distance being measured is between $\frac{1}{4}L_{pp}$ and $\frac{1}{2}L_{pp}$, oversampling occur in which case $\frac{d\phi}{dm} = 2\pi - C$ and L can be written as:

$$L = (2\pi - C)\frac{c}{4\pi f_{rep,sig} n_g}. \quad (5.11)$$

When L is larger than $\frac{1}{2}L_{pp}$, the interference patterns repeat for each $\frac{1}{2}L_{pp}$. We define $L_0 = L \bmod L_{pp}$. The arbitrary distance can be written as:

$$L = \begin{cases} (2N\pi + C)\dfrac{c}{4\pi f_{rep,sig} n_g} & L_0 <= \dfrac{1}{2}L_{pp} \\ (2N\pi - C)\dfrac{c}{4\pi f_{rep,sig} n_g} & L_0 > \dfrac{1}{2}L_{pp} \end{cases}. \tag{5.12}$$

In order to realise an absolute distance measurement, N must be determined properly. Here we use repetition frequency tuning method, which can be easily implemented with the gain-switched frequency comb. After scanning over a certain range of repetition frequencies, a series of C values for different frequencies is obtained. The slope $C = \frac{dC}{df_{rep,sig}}$ is determined with a simple linear fit. A typical sweeping result from 1.1 GHz to 1.4 GHz is shown in Fig. 5.4. In order to avoid aliasing, the repetition frequency of both of the lasers are tuned simultaneously to keep the frequency difference equal to 1 MHz. After the C is calculated, the previous measurement of the distance L_r is written as:

$$L_r = |C|\frac{c}{4\pi n_g}, \tag{5.13}$$

and the integer number N is calculated as:

$$N = round(\frac{L_r}{L_{pp}}). \tag{5.14}$$

After N and C are determined, the absolute distance can be calculated by Eq. 5.12.

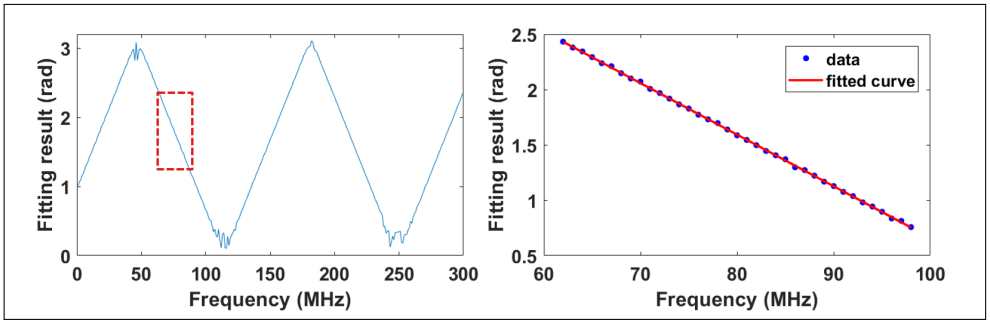

Figure 5.4: (a) A typical sweeping result from 1.1 GHz to 1.4 GHz. (b) The zoom-in figure shows the fitting result, which is used to calculate the absolute distance and determine the integer number N.

5.3.3. ARBITRARY DISTANCE MEASUREMENT

It is obvious from Fig. 5.4 that the fitting results are not correct when C is near zero or π. This problem is also mentioned in [11, 25]. It means that when L is equal to a multiple of $\frac{1}{4}L_{pp}$, a fixed repetition frequency cannot meet measurement requirements. It also means that the measurement accuracy is influenced by distance. In order to realize arbitrary distance measurement, we use Eq. 5.12 at the points, at which C is near π, to

calculate the distance. After tuning the repetition frequency over a certain bandwidth we can always find these points and use the interference patterns with a similar period to calculate the distance. This makes the accuracy independent of the distance when the influence of refractive index is ignored. It should be noted that in order to make sure there are enough points suitable for measurements the tuning bandwidth should be larger than $\frac{c}{L}$. The tuning bandwidth should be larger than the period of the fitting result, to ensure that the points, at which C is close to π, can be found.

5.4. RESULTS AND DISCUSSION

In the experiment, the distances were measured simultaneously with our dual comb system and a fringe counting HeNe interferometer for comparison. Firstly, the carriage was positioned at a distance which is 1 meter longer than the reference arm. This is to ensure that there are enough suitable points for measurement. Subsequently the carriage was moved to 0.5 m. This procedure was repeated for other distances, from 1 m to 2.5 m in steps of 0.5 m. At every position, five measurements were recorded. The environmental conditions (temperature, air pressure and humidity) were recorded simultaneously, and were used for the refractive index calculation using the Edlén Equation [27].

For each repetition frequency around 50 modes are used to calculate the slope C. After tuning the frequency from 1.1 GHz to 1.4 GHz with a step of 1 MHz, about 100 points are used to estimate the final distance with a normal estimation. Fig. 5.5 shows the outcome of this analysis. For each individual measurement the agreement between the dual comb and the HeNe interferometer is within 26 µm. When averaged over five measurements, the largest difference is 12 µm. The standard deviation doesn't show an obvious distance dependence and is on average 6 µm.

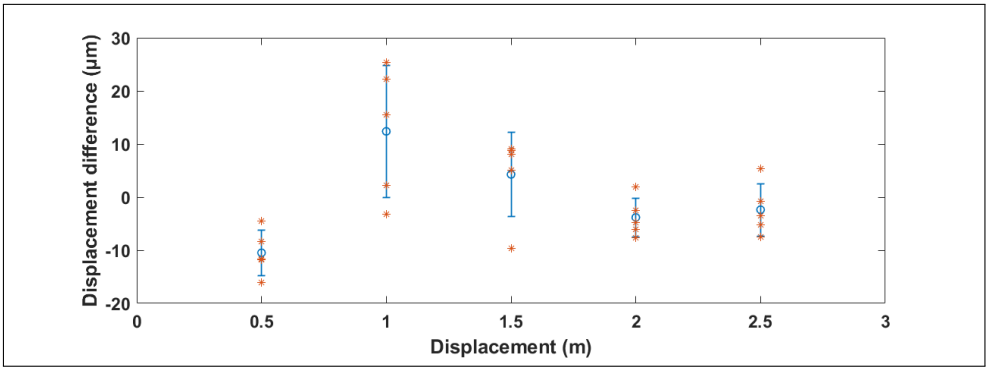

Figure 5.5: The differences between distance measurements taken using a dual comb laser and a HeNe laser interferometry for displacement up to 2.5 m. The error bars show the standard deviation of the measurements.

The linear fitting uncertainty of C is the main limitation for accurate distance measurement. This error mostly arises from the limited number of modes available from the gain switched dual comb. For the dual comb used in this work the spectral bandwidth is around 62.5 GHz (50 modes) in comparison to the measurement with several thousands of modes [11] using a Ti:Sapphire laser. Reducing the repetition frequency of the dual

comb is also a method to increase the number of modes, but this leads to a larger L_{pp}, which in turn reduces the accuracy of the measurement. A smaller L_{pp} means using a finer ruler to measure the distance. Therefore, the best way to improve the accuracy is to extend the bandwidth of the frequency comb. A method of extending the bandwidth of a single gain-switched optical frequency comb has been published [28]. However, this method needs to be further researched to improve the bandwidth of the dual comb.

5.5. CONCLUSION

An absolute distance measurement method for arbitrary distance was presented utilising a discrete component simple cost-efficient dual comb architecture. A comparison measurement with a fringe counting helium-neon (HeNe) laser interferometer has also been implemented. The technique demonstrated absolute arbitrary distance measurement by tuning the repetition frequency of the laser from 1.1 GHz to 1.4 GHz and achieved an accuracy of 12 µm when compared to a He-Ne fringe counting laser interferometer, for a displacement up to 2.5 m. Further improvement on spectral width of the laser source will allow the technique to reach the accuracy obtained with traditional frequency comb sources. This architecture has been photonically integrated [23]. Integration of the required components on to a single chip not only reduces the physical footprint of the device, but simplifies coupling and removes polarisation dependencies. This results in greater device stability and in turn can lead to improvements in the absolute distance measurements.

REFERENCES

[1] K. Hei, K. Anandarajah, E. P. Martin, G. Shi, P. M. Anandarajah, and N. Bhattacharya, *Absolute distance measurement with a gain-switched dual optical frequency comb,* Optics Express **29**, 8108 (2021).

[2] Y.-S. Jang and S.-W. Kim, *Distance measurements using mode-locked lasers: a review,* Nanomanufacturing and Metrology **1**, 131 (2018).

[3] K. Minoshima and H. Matsumoto, *High-accuracy measurement of 240-m distance in an optical tunnel by use of a compact femtosecond laser,* Appl. Opt. **39**, 5512 (2000).

[4] S. A. van den Berg, S. T. Persijn, G. J. P. Kok, M. G. Zeitouny, and N. Bhattacharya, *Many-wavelength interferometry with thousands of lasers for absolute distance measurement,* Physical Review Letters **108** (2012), 10.1103/physrevlett.108.183901.

[5] I. Coddington, W. C. Swann, L. Nenadovic, and N. R. Newbury, *Rapid and precise absolute distance measurements at long range,* Nature Photonics **3**, 351 (2009).

[6] K. Minoshima and H. Matsumoto, *High-accuracy measurement of 240-m distance in an optical tunnel by use of a compact femtosecond laser,* Applied Optics **39**, 5512 (2000).

[7] J. Ye, *Absolute measurement of a long, arbitrary distance to less than an optical fringe,* Opt. Letters **29**, 1153 (2004).

[8] M. Cui, M. G. Zeitouny, N. Bhattacharya, S. A. van den Berg, H. P. Urbach, and J. J. M. Braat, *High-accuracy long-distance measurements in air with a frequency comb laser,* Opt. Letters **34**, 1982 (2009).

[9] K.-N. Joo, Y. Kim, and S.-W. Kim, *Distance measurements by combined method based on a femtosecond pulse laser,* Opt. Express **16**, 19799 (2008).

[10] M. Cui, M. G. Zeitouny, N. Bhattacharya, S. A. van den Berg, and H. P. Urbach, *Long distance measurement with femtosecond pulses using a dispersive interferometer,* Opt. Express **19**, 6549 (2011).

[11] S. A. van den Berg, S. van Eldik, and N. Bhattacharya, *Mode-resolved frequency comb interferometry for high-accuracy long distance measurement,* Scientific Reports **5**, 14661 (2015), article.

[12] J. Lee, Y.-J. Kim, K. Lee, S. Lee, and S.-W. Kim, *Time-of-flight measurement with femtosecond light pulses,* Nature Photonics **4**, 716 (2010).

[13] T.-A. Liu, N. Newbury, and I. Coddington, *Sub-micron absolute distance measurements in sub-millisecond times with dual free-running femtosecond er fiber-lasers,* Opt. Express **19**, 18501 (2011).

[14] J. Lee, S. Han, K. Lee, E. Bae, S. Kim, S. Lee, S.-W. Kim, and Y.-J. Kim, *Absolute distance measurement by dual-comb interferometry with adjustable synthetic wavelength,* Measurement Science and Technology **24**, 045201 (2013).

[15] A. Lešundák, D. Voigt, O. Cip, and S. van den Berg, *High-accuracy long distance measurements with a mode-filtered frequency comb,* Opt. Express **25**, 32570 (2017).

[16] I. Coddington, N. Newbury, and W. Swann, *Dual-comb spectroscopy,* Optica **3**, 414 (2016).

[17] A. J. Metcalf, V. Torres-Company, D. E. Leaird, and A. M. Weiner, *High-power broadly tunable electrooptic frequency comb generator,* IEEE Journal of Selected Topics in Quantum Electronics **19**, 231 (2013).

[18] W. Shieh, H. Bao, and Y. Tang, *Coherent optical ofdm: theory and design,* Optics Express **16**, 841 (2008).

[19] A. D. Ellis and F. G. Gunning, *Spectral density enhancement using coherent wdm,* IEEE Photonics Technology Letters **17**, 504 (2005).

[20] T. Sakamoto, I. Morohashi, and T. Kawanishi, *Mach-zehnder-modulator-based flat comb generator with auto bias control,* in *2008 International Topical Meeting on Microwave Photonics jointly held with the 2008 Asia-Pacific Microwave Photonics Conference* (IEEE, 2008) pp. 154–157.

[21] P. Anandarajah, R. Maher, Y. Xu, S. Latkowski, J. O'carroll, S. Murdoch, R. Phelan, J. O'Gorman, and L. Barry, *Generation of coherent multicarrier signals by gain switching of discrete mode lasers,* IEEE Photonics Journal **3**, 112 (2011).

[22] R. Zhou, S. Latkowski, J. O'Carroll, R. Phelan, L. P. Barry, and P. Anandarajah, *40nm wavelength tunable gain-switched optical comb source,* Optics Express **19**, B415 (2011).

[23] J. K. Alexander, L. Caro, M. Dernaika, S. P. Duggan, H. Yang, S. Chandran, E. P. Martin, A. A. Ruth, P. M. Anandarajah, and F. H. Peters, *Integrated dual optical frequency comb source,* Optics Express **28**, 16900 (2020).

[24] H. Koresawa, K. Shibuya, T. Minamikawa, A. Asahara, R. Oe, T. Mizuno, M. Yamagiwa, Y. Mizutani, T. Iwata, H. Yamamoto, *et al.*, *Lock-in-detection dual-comb spectroscopy,* OSA Continuum **2**, 1998 (2019).

[25] K.-N. Joo and S.-W. Kim, *Absolute distance measurement by dispersive interferometry using a femtosecond pulse laser,* Optics Express **14**, 5954 (2006).

[26] K. Hei, G. Shi, A. Hänsel, Z. Deng, S. Latkowski, S. A. Van den Berg, E. Bente, and N. Bhattacharya, *Distance metrology with integrated mode-locked ring laser,* IEEE Photonics Journal **11**, 1 (2019).

[27] K. Birch and M. Downs, *An updated Edlén equation for the refractive index of air,* Metrologia **30**, 155 (1993).

[28] P. D. Lakshmijayasimha, A. Kaszubowska-Anandarajah, E. P. Martin, P. Landais, and P. M. Anandarajah, *Expansion and phase correlation of a wavelength tunable gain-switched optical frequency comb,* Optics Express **27**, 16560 (2019).

6

DISTANCE MEASUREMENT WITH FREQUENCY SWEEPING INTERFEROMETRY

Distance measurement using frequency sweeping interferometry (FSI) is an absolute distance measurement technique that allows for high accuracy over long distances. Notwithstanding, the measurement accuracy is affected by laser sweeping nonlinearity and limited sweeping range. In this work, an optimized post-processing linearization method is demonstrated to realize high accuracy arbitrary distance measurement using a laser with small modulation range. The interference signal is sparsely resampled to eliminate the influence of the sweeping nonlinearity, and the absolute distance is obtained by analyzing the phase of the resampled signal. In the measurement system, a high finesse Fabry-Perot (F-P) cavity placed in vacuum is used as the measurement reference, so the effect of dispersion mismatch is negligible. Moreover, the distance measurement result is determined by the linear fit of the phase of each resampled point. Therefore, the influence of target vibration and other external random noise can be partially eliminated, and the reliability of the result is high. In the experiment, the sweeping range of the laser source is only 88 GHz. Comparing with a fringe counting interferometer, the standard deviation of the residual errors is 34 μm within a distance of 6.7 m.

Parts of this chapter have been published in Measurement Science and Technology **31** No.4 (2020) [1]

6.1. INTRODUCTION

High accuracy and precision absolute distance measurement is vital to large-scale manufacturing [2, 3], tight-formation flying of satellites [3] and autonomous driving [4]. Distance measurement using frequency sweeping interferometry (FSI) is a promising method because of its high accuracy at long range [5]. Comparing with absolute distance measurement system based on optical frequency comb [6] and high frequency RF system [7], FSI system has characteristics of simple structure and low cost. For a distance measurement system based on FSI, the measured distance L can be estimated by $L = c \cdot \Delta\Phi/(2\pi \cdot B \cdot n_g)$, where B is the optical frequency sweeping range of the laser, $\Delta\Phi$ is the phase change of the interference signal, c is the speed of light in vacuum and n_g is the group refractive index of air [8, 9]. And the theoretical measurement accuracy and precision are subject to the sweeping range and linearity of the laser source [10]. In order to reduce the impact of these two factors on measurement accuracy and precision, there are mainly two signal processing methods are proposed. Each of these two methods has advantages and disadvantages. Therefore, this research proposes a method that overcomes the shortcomings of these two methods at the same time. For the first method, Fabry-Perot (F-P) cavities are generally used to calculate the optical frequency sweeping range B, and the measurement precision can be easily less than 100 kHz. The measurement of $\Delta\Phi$ depends on the measurement of the intensity of the interference signal. Also because the frequency of the interference signal varies over time, it is difficult to realize the high precision measurement of $\Delta\Phi$. This would also lead to the measurement uncertainty of $\Delta\Phi$ being amplified by a large factor. As an example, for a sweep of 50 GHz in a laser of wavelength 600 nm, the amplification factor is about 10000 [11]. So the major contributor to the final measurement uncertainty arises from the impreciseness of $\Delta\Phi$. The nonlinearity of the optical frequency sweeping and the vibration of the target will seriously affect the measurement accuracy of $\Delta\Phi$. Adding a compensation system into the instrument can reduce the effect of target vibration, but this increases the complexity of the instrument[12]. Eliminating the effect of target vibration without increasing complexity is also a worthwhile topic to investigate. Kalman filter techniques are also proposed to compensate the measurement errors caused by low frequency vibration of the target [13–15] and sweeping nonlinearity of the laser [16]. However, for random vibration of the target or mode hopping of the laser, this method would not be very appropriate.

The second method called frequency-sampling method is a recognized post-processing scheme. In 2011, Baumann et al. used a femtosecond optical frequency comb as an optical frequency standard to resample the interference signal at equal frequency steps [17, 18], and demonstrated a precision of 10 µm at a distance of 10.5 m. A fiber Mach–Zehnder Interferometer is a more cost effective choice in the frequency-sampling method [19] instead of a optical frequency comb. Hao Pan et al. added an hydrogen cyanide (HCN) cavity to the laser distance measurement system and used multiple signal classification (MUSIC) algorithm to enhance the measurement precision to 45 µm within 8 m [20]. Cheng Lu et al. added a laser Doppler velocimetry (LDV) component to the measurement system to compensate for the environmental vibration. The measurement uncertainty of 8.6 µm + 0.16 µm/m · L (k = 2) with a measuring range from 1 m to 24 m was achieved [21]. In order to satisfy the Nyquist sampling theorem, the optical path difference of the Mach–Zehnder interferometer should be at least twice that of the mea-

suring interferometer. The increase in measuring range, necessitates that the length of the optical fiber must be increased accordingly, resulting in the effects of fiber jitter [22] and dispersion becoming more significant. Hao Pan [20] and Guodong Liu [23], proposed different algorithms to eliminate the dispersion mismatch. In this chapter, we propose an optimized post-processing method and an FSI system for absolute distance measurement with an F-P cavity as the measurement reference. Compared with a fiber Mach–Zehnder interferometer, the F-P cavity is more stable and traceable. And because the F-P cavity is placed in vacuum, the problem of dispersion mismatch does not exist for the distance measurement system. Although, the interference signal is sparsely resampled, arbitrary distance is obtained with only one F-P cavity. The measurement result is determined by the linear fit of the phase of each resampled point. So the influence of target vibration and other external random noise can be partially eliminated, and the reliability of the result is higher than a traditional FSI system. In the experiment, the sweeping range of the tunable laser is only 88 GHz. Comparing with a commercial fringe counting interferometer, the standard deviation of the residual errors of 34 μm with the measuring range from 2200 mm to 6700 mm has been shown.

6.2. MEASUREMENT PRINCIPLES

The distance measurement technique we propose and demonstrate in this work is based on FSI. An external cavity diode laser (ECDL) is used as the optical frequency sweeping laser source. And a F-P cavity is used to generate the periodic maxima to resample the interference signal from the measurement interferometer. This measurement is then compared with a commercial fringe counting interferometer.

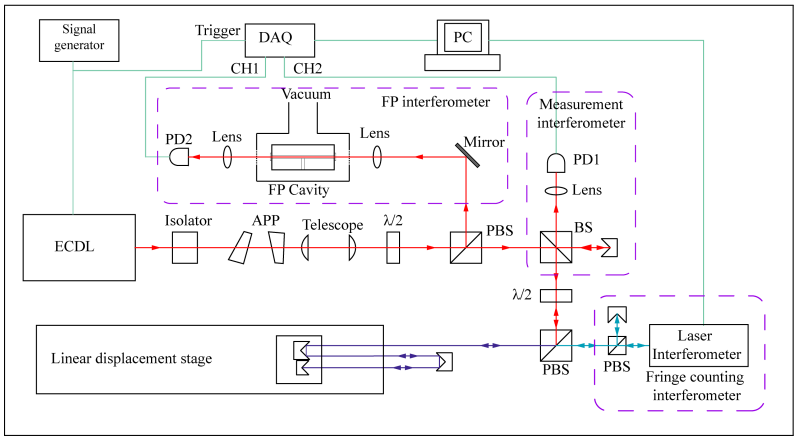

Figure 6.1: Schematic of the experimental setup of FSI system for absolute distance measurement. ECLD: external cavity laser diode, APP: anamorphic prism pair, BS: beam-splitter, PBS: polarizing beam-splitter, DAQ: data acquisition, PD: photo detector.

Fig. 6.1 illustrates the schematic of the proposed FSI for absolute distance measurement. This system mainly consists of five parts: a tunable laser source, an F-P interferometer, a measurement Michelson interferometer, a commercial fringe counting inter-

ferometer and a control & DAQ system. Directly after the ECDL and the optical isolator, a few optical components prepare the beam for use in the rest of the setup. After the initial beam-shaping, the light is divided into two paths using a polarizing beam splitter. The half-wave-plate placed before the beam splitter can be rotated to vary the splitting ratio between the F-P interferometer and the measurement interferometer the rest. The measurement interferometer is a typical Michelson with photodetector 1 (PD1) measuring its output. Similarly PD2 measures the output of the F-P interferometer. The beat signal detected by the PD1 at the output from the measurement interferometer can be expressed as:

$$I(\upsilon) = I_0 \cos(2\pi \cdot D \cdot n \cdot \upsilon / c), \tag{6.1}$$

where I_0 denotes the amplitude of the interference signal, υ denotes the instantaneous optical frequency, D denotes the optical path difference of the measurement interferometer, n denotes the phase refractive index of air for a wavelength of $\lambda = c/\upsilon$ and c is the velocity of light in vacuum.

Sweeping nonlinearity of laser results in nonlinearity of υ and time. Thus, the signal of measurement interferometer acquired by DAQ is not a fixed frequency cosine signal. This is the main reason why the nonlinearity of laser leads to the decrease of measurement accuracy. Defining the argument of the cosine of Eq.6.1 as

$$\phi = 2\pi \cdot D \cdot n \cdot \upsilon / c, \tag{6.2}$$

And taking the derivative with respect to frequency we get

$$\frac{d\phi}{d\upsilon} = \frac{2\pi D}{c(\frac{dn2\pi D}{d\upsilon c_g})}, \tag{6.3}$$

where the group refractive index n_g is defined as [24]

$$n_g = n + \upsilon \frac{dn}{d\upsilon}. \tag{6.4}$$

Then the length to be measured L is only determined from the slope $\frac{d\phi}{d\upsilon}$ [25] as

$$L = \frac{D}{2} = \frac{d\phi}{d\upsilon} \cdot \frac{c}{4\pi n_g}. \tag{6.5}$$

Since $I(\upsilon)$ represents a function of instantaneous optical frequency υ if it is resampled with equal optical frequency intervals $\Delta\upsilon$ the effect of laser sweeping nonlinearity will be eliminated. The measurement signal would become

$$I(p)=\mathrm{I}_0 \cos(\frac{d\phi}{d\upsilon}\Delta\upsilon \cdot p + \phi_0) = I_0 \cos(\frac{4\pi \cdot n_g \cdot L \cdot \Delta\upsilon}{c} \cdot p + \frac{4\pi \cdot n_0 \cdot L \cdot \upsilon_0}{c}) \tag{6.6}$$

where p = 1, 2, ..., N, and N represents the total number of sampling points, υ_0 denotes the initial optical frequency, n_0 denotes the phase refractive index of the laser with initial optical frequency. For the F-P interferometer, the difference between two successive resonance frequencies, the free spectral range (FSR) $\Delta\upsilon_{FSR}$ [26] is given by the equation below,

$$\Delta v_{FSR} = \frac{c}{2 \cdot n \cdot d_{FP}} \tag{6.7}$$

where d_{FP} denotes the length of the F-P cavity.

F-P resonance peaks can be used to sample the interference signal with optical frequency intervals equal to the FSR. According to the requirement of frequency sampling method, the signals of PD1 and PD2 are sampled synchronously. Then, the measurement interference signal could be further sampled at Δv_{FSR}, which is calculated as

$$I(i) = I_0 \cos(\frac{4\pi \cdot n_g \cdot L \cdot \Delta v_{FSR}}{c} \cdot i + \frac{4\pi \cdot n_0 \cdot L \cdot v_0}{c}) \tag{6.8}$$

here Δv_{FSR} denotes the FSR of the F-P cavity, i = 1, 2, …, N, and N denotes the total number of sampling points. Using d_{FP}, the length of the F-P cavity we can rewrite the above equation as

$$I(i) = I_0 \cos(\frac{2\pi \cdot n_g \cdot L}{d_{FP}} \cdot i + \frac{4\pi \cdot n_g \cdot L \cdot v_0}{c}) \tag{6.9}$$

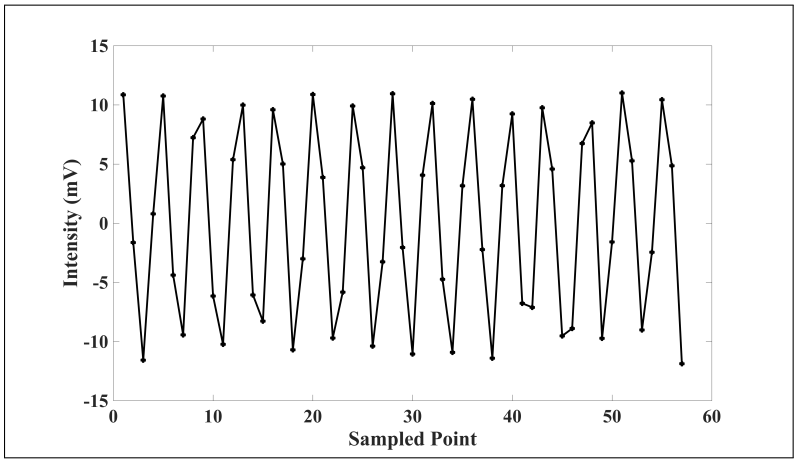

Figure 6.2: The resampled signal.

Fig. 6.2 shows the resampled signal. We performed Hilbert transform on the resampled signal to obtain the instantaneous phase. I(i) is the resampled signal of the measurement interference signal. We denote $\tilde{I}$(i) is the Hilbert transform of I(i). Then the phase of I(i) can be expressed as

$$\phi(i) = \arctan \frac{I(i)}{\tilde{I}(i)}. \tag{6.10}$$

After unwrapping the phase $\phi(i)$, we obtain $\acute{\phi}(i)$. Then taking the derivative of $\acute{\phi}(i)$ with respect to i we get the frequency f_I.

$$f_I = \frac{d\phi(i)}{di}. \tag{6.11}$$

f_I is dimensionless and the range is from 0 to 0.5.

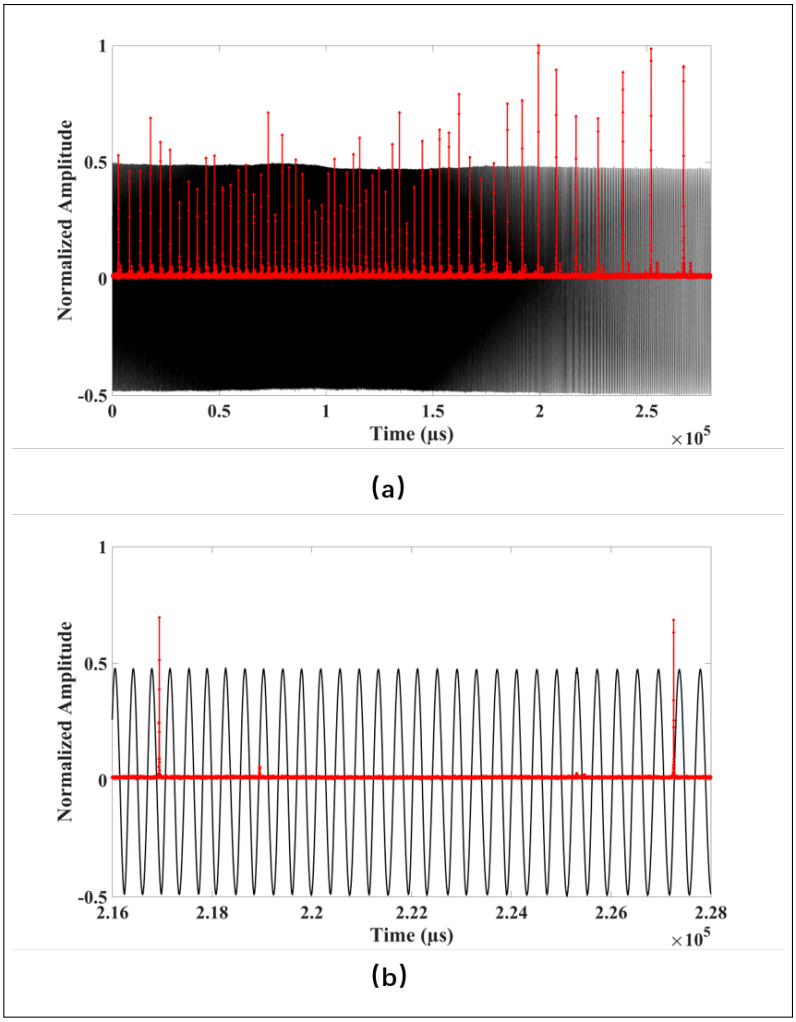

Figure 6.3: Interference signal of measurement interferometer (black) and F-P interferometer (red). (a) The signal of one measurement. (b) Enlarged detail of (a) showing fringes between the F-P resonances.

The length of the F-P cavity is limited, if the measured distance is larger than the length of the F-P cavity, under sampling would occur, which is shown in Fig. 6.3. And this leads to an ambiguous measurement result. In order to realize the measurement of arbitrary distance, we set M_{ean} as the average number of peaks and valleys of the measurement interferometer signal between every two peaks of the F-P interferometer

signal in a single measurement. The absolute distance of the target can be obtained by

$$L = \begin{cases} (0.5 \cdot m + f_I) \cdot d_{FP} / n_g & when\ m\ is\ an\ even\ number\ or\ zero \\ (0.5 \cdot (m+1) - f_I) \cdot d_{FP} / n_g & when\ m\ is\ an\ odd\ number \end{cases}, \tag{6.12}$$

where m is an integer, and $(M_{ean} - 1) < m \leq M_{ean}$. f_I is the frequency of the resampled interference signal.

The uncertainty of the FSI system uL can be obtained from eq.6.12 as

$$u_L = \begin{cases} \sqrt{(\frac{0.5 d_{FP}}{n_g} \cdot u_m)^2 + (\frac{0.5m + f_I}{n_g} \cdot u_{dFP})^2 + (\frac{d_{FP}}{n_g} \cdot u_{f_I})^2 + (\frac{0.5 \cdot m \cdot d_{FP} + f_I \cdot d_{FP}}{n_g^2} \cdot u_{n_g})^2} \\ when\ m\ is\ an\ even\ number\ or\ zero \\ \sqrt{(\frac{0.5 d_{FP}}{n_g} \cdot u_m)^2 + (\frac{0.5m + 0.5 - f_I}{n_g} \cdot u_{dFP})^2 + (\frac{d_{FP}}{n_g} \cdot u_{f_I})^2 + (\frac{0.5 \cdot (m+1) \cdot d_{FP} - f_I \cdot d_{FP}}{n_g^2} \cdot u_{n_g})^2} \\ when\ m\ is\ an\ odd\ number \end{cases}. \tag{6.13}$$

The major contributor to the final uncertainty is the uncertainty of f_I and d_{FP}. Because m is an integer, the uncertainty of m is 0. And in the laboratory environment, the uncertainty of n_g is small enough to be neglected. Therefore Eq.6.13 can be simplified to

$$u_L = \begin{cases} \sqrt{(\frac{0.5m + f_I}{n_g} \cdot u_{dFP})^2 + (\frac{d_{FP}}{n_g} \cdot u_{f_I})^2} & when\ m\ is\ an\ even\ number\ or\ zero \\ \sqrt{(\frac{0.5m + 0.5 - f_I}{n_g} \cdot u_{dFP})^2 + (\frac{d_{FP}}{n_g} \cdot u_{f_I})^2} & when\ m\ is\ an\ odd\ number \end{cases}. \tag{6.14}$$

In our laser distance measurement system, the sweeping range of the ECDL being only 88 GHz the number of resonances from the F-P cavity overlapping with the measured signal is only 58, which is shown in Fig. 6.3. Thus, the length of the resampled signal is only 58 points. Fig. 6.2 shows the resampled signal. We performed Hilbert transform on the resampled signal to obtain the instantaneous phase which is shown in Fig. 6.2. After unwrapping the phase, we perform a least-squares fit to the phase curve to obtain the fitted curve as shown in Fig. 6.5. The resolved phase is shown in black, and the result of least square fitting of the phase is in red. The slope of the fitted line is 1.625±0.004, with 95% confidence bounds. The frequency of the signal shown in Fig. 6.5, is calculated to be $f_I = 0.2586 \pm 0.00064$, again with 95% confidence bounds. Then the group refractive index is ng = 1.0002656, the absolute distance of the target can be calculated for Eq. 6.12, $L = (0.5 \cdot m + f_I) \cdot d_{FP} / n_g = (0.5 \times 52 + 0.2586) \times 101.768 / 1.0002656 = 2671.576 \pm 0.065 mm$. For a traditional FSI system, the measured distance L is estimated by $L = c \cdot \Delta\Phi(2\pi \cdot B \cdot n_g)$.The measurement accuracy is determined by the measurement accuracy of B and $\Delta\Phi$. The measurement of B and $\Delta\Phi$ at the starting and ending positions of laser sweeping greatly affect the reliability of measurement. And the influence of

vibration on distance measurement is amplified by a large amplification factor [11]. For our method the result we obtain from Fig. 6.5 is determined by all the resampled points, and the measurement error at each point is reduced by averaging. In addition, according to Eq. 6.13 the influence of vibration on distance measurement accuracy depends on $(d_{FP}/n_g)\cdot u_{f_l}$, which is not amplified. Thus the measurement error is not amplified.

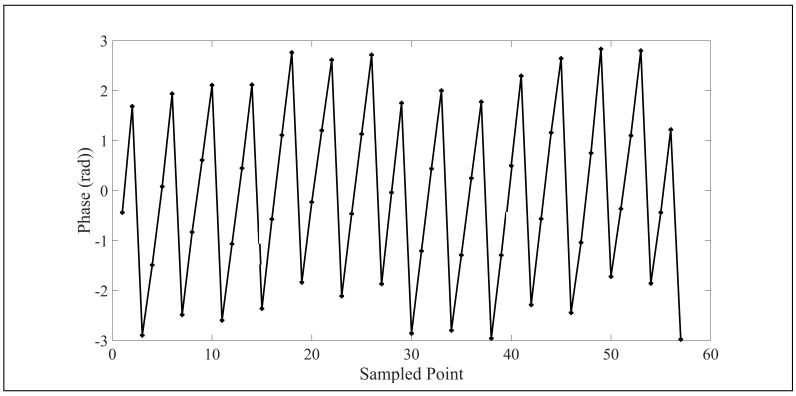

Figure 6.4: The phase obtained from the Hilbert transform of the resampled signal which is shown in Fig. 6.2.

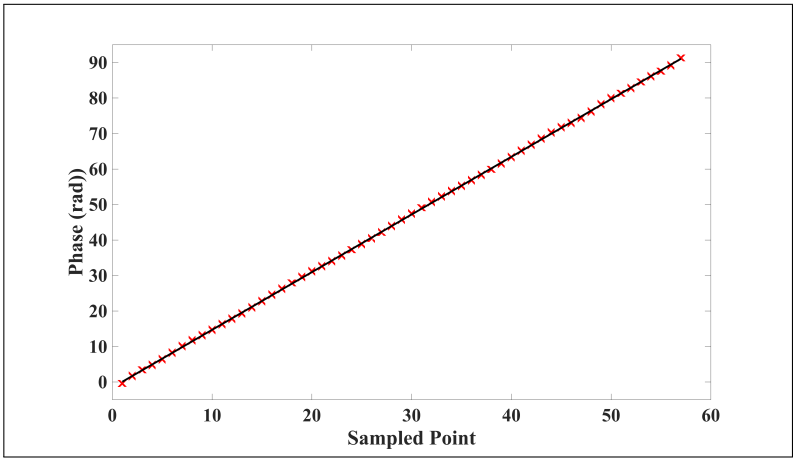

Figure 6.5: The phase after unwrapping (black) fitted using the least squares function (red).

6.3. EXPERIMENT

Fig. 6.1 illustrates the schematic diagram of the actual experimental FSI system. In this system, an ECDL (New Focus TLB-6210) is chosen as the tunable laser source with the central wavelength of 633nm, and the sweeping range available is 88GHz. The anamorphic prism pair and the telescope are employed to change the elliptical beam cross-section of the laser diode into a circular one, and to improve the collimation of the

measurement beam. The signal generator is employed to supply the sweeping signal at the frequency of 2 Hz. The F-P cavity (custom built, Research Electro-Optics, finesse is 11041) is made out of ultra-low expansion (ULE) glass and is placed in vacuum. The free spectral range (FSR) of the F-P cavity was calibrated before the experiment. The length of the FP cavity dFP is calculated by $d_{FP} = c/2n \cdot FSR = 101.768$ mm.

The Michelson measurement interferometer is an unbalanced interferometer built with 1 inch sized optics, using a non-polarizing beam splitter (BS) and retroreflector prisms, whose long arm is used as the length to be measured. The measurement arm has a maximum length of 1.5 m and consists of a long rail with electric carriage carrying two retroreflector prisms. As is shown in Fig. 6.1, The measured optical path is folded three times by 3 retroreflector prisms. At the nearest measurement position of the rail, the distance difference of the two arms of the measurement interferometer is 2208.877 mm. This position is set to be measurement origin of the fringe counting interferometer. The commercial fringe counting interferometer (Agilent 5519A), with a linear distance measurement accuracy of ± 0.4 ppm in air is used for the comparison measurement.

The beam from the ECLD and the fringe counting interferometer is combined with a polarizing beam-splitter (PBS). The auxiliary mirrors in the optical path are adjusted to ensure that the two beams overlap optimally. As a result, both beams largely propagate through the same volume of air, having a shared measurement arm. Then the half-wave-plate is employed to separate the returning beams after the PBS. The laser from the fringe counting interferometer propagates back through the same path to the fringe counting interferometer which contains the detector for fringe counting. The interferometer signal of the Michelson measurement interferometer is detected by PD1. The detected signal of PD1 and PD2 are synchronously sampled by a DAQ board. The bit-with of the DAQ board is 22bit and the sampling rate is 1MHz.

In the experiment, the carriage was physically moved from 0 mm to 1500 mm, corresponding to an optical path length of 0 mm to 4500 mm. At each position 10 measurements were made. Moreover, the displacement of the carriage was measured by both FSI system and the fringe counting interferometer simultaneously. During the experiment, environmental conditions were measured by a VAISALA air parameter sensor. The temperature, humidity and atmospheric pressure were measured to be 27±0.2 °C, 46.2±0.2% and $101.61 \pm 0.02 kPa$.

6.4. RESULTS AND DISCUSSION

In the experiment, the F-P cavity is located inside a small vacuum vessel and has large thermal mass so the fluctuation in the temperature of the cavity is low. Thus the effect of temperature on FSR is small enough to be ignored. The uncertainty of air pressure in the small vacuum vessel is 0.05 kPa. Substituting temperature and humidity parameters, calculate by using Edlén Equation, the uncertainty of the refractive index in the F-P cavity is un = 0.00000013, the uncertainty of FSR is u_{FSR} = 180 Hz. Assuming n_g = 1, from Eq. 6.7 the uncertainty of physical length of the cavity (with coverage factor of k = 2) is u_{dFP} = 0.00013 mm.

The absolute distances obtained from the FSI system vary from about 2200 mm to 6700 mm. The range of m in Eq. 6.12 and 6.14 is from 43 to 131. The measurement uncertainty of the resampled frequency is u_{f_I} = 0.0007 (with coverage factor of k = 2). At

each position, substituting n_g=1.0002656, m = 43 ~ 131, u_{dFP} = 0.00013 mm and u_{f_I} = 0.0007 into the Eq.6.14 gives u_L = 71.3 ~ 71.7 µm (with coverage factor of k = 2). Table. 6.1 shows the uncertainty contributions of d_{FP} and f_I.

Because the value of m is not large, the contribution to measurement uncertainty of u_{dFP} is small. The main uncertainty contribution is u_{f_I}. Path length changes due to vibrations, uncertainty in refractive index of air, the inaccuracy of resampling position and the intensity instability of the ECDL are the main reasons that result in the measurement uncertainty in the determination of f_I. If the sweeping range of the ECDL was enlarged, more resampled points could be obtained and smaller measurement uncertainty could be obtained.

Table 6.1: Measurement uncertainty budget according to Eq.6.14

Quantity	Uncertainty	Uncertainty contribution
d_{FP}	$0.00013mm$	$2.8 \sim 8.6\mu m$
f_I	0.0007	$71.2\mu m$
Combined expanded uncertainty (with coverage factor of k = 2)		$u_L = 71.3 \sim 71.7\mu m$

The residual error between the individual measurements done by FSI system and the fringe counting interferometer is shown in Fig. 6.6. The central wavelength of the ECDL and the wavelength of the fringe counting interferometer are both 633 nm so the refractive index is assumed to be to the same in their ranging formulas. The zero position is based on the average of 10 measurements. For each individual measurement, the agreement between the FSI system and the fringe counting interferometer is within 100 µm. When averaged over ten measurements, the largest difference is 28 µm. The standard deviation does not show a clear distance dependence and is on average 34 µm. Because environmental effects such as turbulence and vibrations will affect a single measurement result, averaging multiple measurements can improve the measurement accuracy and precision.

As mentioned above, arbitrary distances are chosen, but path length differences very close to L_d = 0 or $L_d = d_{FP}/4$ are avoided. At L_d = 0 m all wavelengths have the same phase (neglecting nonlinear air dispersion), so a typical cosine dependence like in Fig. 6.3 is not observed. Close to $L_d = d_{FP}/4$ the Nyquist frequency is approached and each period of the cosine is only determined by 2 points. In order to overcome the issue, a multiplex scheme could be envisaged. We can add another reference path to the measurement interferometer. By using a beam splitter and two shutters, then the reference path can be always selected such that the path length differences close to L_d = 0 or $L_d = d_{FP}/4$ do not occur.

6.5. CONCLUSION

In this chapter, we have proposed a method that substantially reduces the negative impacts of sweeping linearity, and absolute distance measurement result is obtained from the sparsely resampled signal. This method employs just one F-P cavity as the measurement reference to realize high accuracy arbitrary distance measurement. Compared to

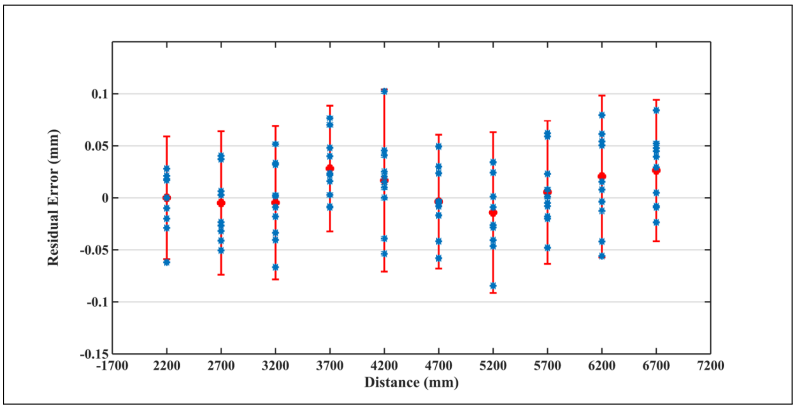

Figure 6.6: The difference between distance measurement with the FSI system and the fringe counting interferometer. The red bar denotes twice of the standard deviation of the measurements.

techniques using Mach-Zehnder interferometers, the F-P cavity is more stable and traceable. The F-P cavity being in vacuum, dispersion mismatch is avoided. Moreover, Hilbert transform algorithm and least square method are used to calculate the frequency of the resampled signal, which lead to an averaging effect in the analysis. Therefore, the influence of target vibration and other external random noise can be partially eliminated, and the reliability of the result is higher than a traditional FSI system. In the experiment, an ECDL with modulation range of 88GHz is used as the laser source. When compared with measurements done with a fringe counting interferometer, the standard deviation of the residual errors is 34 µm. Sparsely resampling and smaller sweeping range are beneficial to reducing the processing cost and improving measurement efficiency. This method makes FSI system for absolute distance measurement more practical.

REFERENCES

[1] G. Shi, K. Hei, W. Wang, and N. Bhattacharya, *High-precision frequency sweeping interferometry for absolute distance measurement using a tunable laser with sweeping range of 88 ghz,* Measurement Science and Technology **31**, 045201 (2020).

[2] B. Muralikrishnan, S. Phillips, and D. Sawyer, *Laser trackers for large-scale dimensional metrology: A review,* Precision Engineering **44**, 13 (2016).

[3] I. Coddington, W. C. Swann, L. Nenadovic, and N. R. Newbury, *Rapid and precise absolute distance measurements at long range,* Nature Photonics **3**, 351 (2009).

[4] R. Komissarov, V. Kozlov, D. Filonov, and P. Ginzburg, *Partially coherent radar unties range resolution from bandwidth limitations,* Nature communications **10**, 1 (2019).

[5] B. L. Swinkels, *High accuracy absolute distance metrology,* in *ESA Special Publication*, Vol. 621 (2006).

[6] R. Yang, F. Pollinger, K. Meiners-Hagen, M. Krystek, J. Tan, and H. Bosse, *Absolute distance measurement by dual-comb interferometry with multi-channel digital lock-in phase detection,* Measurement Science and Technology **26**, 084001 (2015).

[7] J. Guillory, M. T. de la Serve, D. Truong, C. Alexandre, and J.-P. Wallerand, *Uncertainty assessment of optical distance measurements at micrometer level accuracy for long-range applications,* IEEE Transactions on Instrumentation and Measurement **68**, 2260 (2019).

[8] Z. Liu, Z. Liu, Z. Deng, and L. Tao, *Interference signal frequency tracking for extracting phase in frequency scanning interferometry using an extended kalman filter,* Applied optics **55**, 2985 (2016).

[9] M. Medhat, M. Sobee, H. Hussein, and O. Terra, *Distance measurement using frequency scanning interferometry with mode-hoped laser,* Optics & Laser Technology **80**, 209 (2016).

[10] T. DiLazaro and G. Nehmetallah, *Large-volume, low-cost, high-precision fmcw tomography using stitched dfbs,* Optics Express **26**, 2891 (2018).

[11] A. P. Cabral and J. M. Rebordão, *Accuracy of frequency-sweeping interferometry for absolute distance metrology,* Optical Engineering **46**, 073602 (2007).

[12] A. P. Cabral, M. A. Abreu, and J. M. Rebordão, *Dual-frequency sweeping interferometry for absolute metrology of long distances,* Optical Engineering **49**, 085601 (2010).

[13] X. Jia, Z. Liu, L. Tao, and Z. Deng, *Frequency-scanning interferometry using a time-varying kalman filter for dynamic tracking measurements,* Optics Express **25**, 25782 (2017).

[14] L. Tao, Z. Liu, W. Zhang, and Y. Zhou, *Frequency-scanning interferometry for dynamic absolute distance measurement using kalman filter,* Optics letters **39**, 6997 (2014).

[15] X. Jia, Z. Liu, Z. Deng, W. Deng, Z. Wang, and Z. Zhen, *Dynamic absolute distance measurement by frequency sweeping interferometry based doppler beat frequency tracking model,* Optics Communications **430**, 163 (2019).

[16] Z. Deng, Z. Liu, B. Li, and Z. Liu, *Precision improvement in frequency-scanning interferometry based on suppressing nonlinear optical frequency sweeping,* Optical Review **22**, 724 (2015).

[17] E. Baumann, F. R. Giorgetta, I. Coddington, L. C. Sinclair, K. Knabe, W. C. Swann, and N. R. Newbury, *Comb-calibrated frequency-modulated continuous-wave ladar for absolute distance measurements,* Optics letters **38**, 2026 (2013).

[18] E. Baumann, F. R. Giorgetta, J.-D. Deschênes, W. C. Swann, I. Coddington, and N. R. Newbury, *Comb-calibrated laser ranging for three-dimensional surface profiling with micrometer-level precision at a distance,* Optics Express **22**, 24914 (2014).

[19] T. Hariyama, P. A. Sandborn, M. Watanabe, and M. C. Wu, *High-accuracy range-sensing system based on fmcw using low-cost vcsel,* Optics Express **26**, 9285 (2018).

[20] H. Pan, X. Qu, and F. Zhang, *Micron-precision measurement using a combined frequency-modulated continuous wave ladar autofocusing system at 60 meters standoff distance,* Optics Express **26**, 15186 (2018).

[21] C. Lu, G. Liu, B. Liu, F. Chen, and Y. Gan, *Absolute distance measurement system with micron-grade measurement uncertainty and 24 m range using frequency scanning interferometry with compensation of environmental vibration,* Optics Express **24**, 30215 (2016).

[22] L. Tao, Z. Liu, W. Zhang, Z. Liu, and J. Hong, *Real-time drift error compensation in a self-reference frequency-scanning fiber interferometer,* Optics Communications **382**, 99 (2017).

[23] L. Guodong, X. Xinke, L. Bingguo, C. Fengdong, H. Tao, L. Cheng, and G. Yu, *Dispersion compensation method based on focus definition evaluation functions for high-resolution laser frequency scanning interference measurement,* Optics Communications **386**, 57 (2017).

[24] S. A. van den Berg, S. van Eldik, and N. Bhattacharya, *Mode-resolved frequency comb interferometry for high-accuracy long distance measurement,* Scientific Reports **5**, 14661 (2015), article.

[25] S. A. van den Berg, S. T. Persijn, G. J. P. Kok, M. G. Zeitouny, and N. Bhattacharya, *Many-wavelength interferometry with thousands of lasers for absolute distance measurement,* Physical Review Letters **108** (2012), 10.1103/physrevlett.108.183901.

[26] A. Lešundák, D. Voigt, O. Cip, and S. van den Berg, *High-accuracy long distance measurements with a mode-filtered frequency comb,* Optics Express **25**, 32570 (2017).

7

CONCLUSION AND OUTLOOK

7.1. CONCLUSION

Distance metrology based on the optical frequency comb (OFC) is a good solution to the demands of high-accuracy long-distance measurement. In Chapter 1, the background knowledge which is necessary for this thesis is introduced. OFC is the key component which brings distance metrology systems to higher accuracies thus the evolution of the OFC is introduced first. Having a previous knowledge of other laser distance metrology techniques is helpful for understanding the methods developed using the OFC. Since OFC was invented at the beginning of the century, several methods have been developed. In Chapter 2, some typical interferometry methods are introduced in detail and their advantages and disadvantages are discussed. These methods can realise high-accuracy long distance measurements but there are still some challenges that need to be overcome. Refractive index of air is one of them, which has to be carefully considered in distance measurements. Especially when using OFC, which is a multi-wavelength laser sourse, the dispersion caused by refractive index needs to be compensated properly. In Chapter 3, a compensation method is demonstrated for the spectrally resolved technique to eliminate the influence of dispersion on measurement accuracy. The other challenge is the price and size of measurement system. A cheap and compact distance metrology solution is very important for industrial applications. Until now, to my knowledge, there is no commercial rangefinder, which is based on OFC. The large size, complex configuration and high price are the bottlenecks restricting OFC's introduction in industry. In this thesis, we tested smaller and potentially lower cost OFC's for their suitability in realising distance metrology. Three different methods using OFC and tunable laser are shown in Chapter 4, Chapter 5 and Chapter 6.

In Chapter 3, a dispersion compensation method is demonstrated to improve the accuracy of distance measurement based on spectrally resolved interferometry. It shows an agreement within 500 nm for a distance up to 50 metres when compared with a conventional He-Ne fringe counting interferometer. The limitations of this method are the uncertainty of refractive index of air and the accurate determination of the intensities of the modes.

In Chapter 4, the distance measurement result is shown with an integrated mode-locked laser. The spectrally resolved images are obtained with a Virtually Imaged Phased Array spectrometer. The distance derived shows a deviation of 6 µm from the reference, for a distance up to 25 mm. This is significant for frequency comb-based distance measurement. The cost of laser, energy consumption and footprint are extremely reduced, which could enable a wide range of applications for which current frequency comb systems are too bulky and expensive. However, spectral width and coherence of integrated mode-locked laser need to be further improved to meet the high-accuracy and long distance demands of industrial and other applications.

In Chapter 5, an absolute distance measurement method for arbitrary distance is demonstrated using mode-resolved spectral interferometry with a gain-switched dual comb. An accuracy of 12 µm for a displacement up to 2.5 m is demonstrated , when compared to a He-Ne fringe counting laser interferometer, by tuning the repetition frequency of the dual comb from 1.1 GHz to 1.4 GHz. Compared to the single comb method, dual comb measurement system reduces the complexity of the setup. The gain-switched dual comb, which can be photonically integrated, is a good solution for a cheap and small size OFC laser source.

In Chapter 6, an absolute distance measurement technique with frequency sweeping interferometry is demonstrated. The interference signal is resampled with high finesse Fabry-Perot cavity placed in vacuum, which eliminate the influence of the sweeping nonlinearity. This method successfully obtain a series of interference signal in time domain, which is similar to an optical frequency comb. Compared with a fringe counting interferometer, the standard deviation of the residual errors is 34 µm within a distance of 6.7 m with the 88 GHz sweeping range of the laser source. If the sweeping range can be further expanded, this method can achieve the accuracy similar to optical frequency comb.

In this thesis, there are three main concepts: the optical frequency comb (OFC), the distance metrology technology and industrial applications. When only focusing on distance measurements with OFC, the accuracy is the most important parameter of measurement system. To achieve the high and accurate results, the finest ruler should be used to measure the distance. In our research, when using OFC and interferometry to do distance metrology the finest ruler is the wavelength of each mode. The refractive index of air should be also properly accounted for and measured when measuring distance in the air. However, when combined with industrial applications the problem becomes more complex. The size and cost of measurement setup is very important for industrial applications. The specific applications may also have special demands. Integrated optics based combs are proving to be the most useful and efficient technique to reduce the cost and size of the measurement system. Each type of OFC with its own generating method has their drawbacks and benefits. For example the OFC generated with gain-switched method has a narrow bandwidth, but the repetition frequency can be easily tuned, which is very significant for absolute distance measurement. The integrated mode-locked ring laser made an OFC with broader bandwidth possible, but the coherence of the pulses need to be further improved for long distance measurement. In conclusion, the measurement methods and types of OFC should be properly developed based on the applications. A stable and broad bandwidth OFC is important and sig-

nificant for high accuracy measurements. Further development of compact OFC's with suitable attributes is necessary to take the accuracies offered by these lasers to industry.

7.2. OUTLOOK

In this thesis, the main has been spent in looking for a proper method to reduce the size and cost of the distance metrology setup based on OFC. The techniques to improve the measurement accuracy with disperson correction is investigated. However, the measurement speed is also an important aspect, especially for optical sensing [1, 2], imaging [3, 4] and vibration measurement [5, 6]. Many methods have been used to do OFC based distance measurement, such as dual comb techniques [7], correlation Fourier transform based techniques [8] and mode-resolved interferometry [9]. The fastest method is dual comb, which can complete a measurement in several milliseconds[7], but this is still not fast enough for dynamic measurement. The integration time, which is relative to the repetition frequency difference, limits the measurement speed.

Compressive sensing (CS) is an exciting, rapidly developing field which has attracted considerable attention in signal processing, communication technology and imaging processing [10]. Recently CS has been applied in many frequency comb applications, such as ultrafast microscopy [11] and spectroscopy [12]. Using CS technique the spectrum of OFC can be recovered in several measurements, which can promote speed of measurement dramatically.

Future work should investigate efficient sampling matrices which can dramatically reduce measurements. Random matrix is a universal choice, but sometimes it is not the best. In our case the signal is very sparse, so a good matrix is necessary for improving the measurement speed. The other important aspect is the method of sampling the frequency comb with selected matrix. There are several methods published in recent years, such as the modulation method with SLM [13]. If the comb is first dispersed, an electro-optic modulator can also modulate the comb [14].

REFERENCES

[1] J. Guo, Y. Ding, X. Xiao, L. Kong, and C. Yang, *Multiplexed static fbg strain sensors by dual-comb spectroscopy with a free running fiber laser,* Optics Express **26**, 16147 (2018).

[2] N. Kuse, A. Ozawa, and Y. Kobayashi, *Static fbg strain sensor with high resolution and large dynamic range by dual-comb spectroscopy,* Optics Express **21**, 11141 (2013).

[3] E. Hase, T. Minamikawa, T. Mizuno, S. Miyamoto, R. Ichikawa, Y.-D. Hsieh, K. Shibuya, K. Sato, Y. Nakajima, A. Asahara, *et al., Scan-less confocal phase imaging based on dual-comb microscopy,* Optica **5**, 634 (2018).

[4] H. Zhao, Z. Zhang, X. Xu, H. Zhang, J. Zhai, and H. Wu, *Three-dimensional imaging by frequency-comb spectral interferometry,* Sensors **20**, 1743 (2020).

[5] W. Yu, P. Pfeiffer, A. Morsali, J. Yang, and J. Fontaine, *Comb-calibrated frequency*

sweeping interferometry for absolute distance and vibration measurement, Optics letters **44**, 5069 (2019).

[6] J. E. Posada-Roman, J. A. Garcia-Souto, D. A. Poiana, and P. Acedo, *Fast interrogation of fiber bragg gratings with electro-optical dual optical frequency combs,* Sensors **16**, 2007 (2016).

[7] I. Coddington, W. C. Swann, L. Nenadovic, and N. R. Newbury, *Rapid and precise absolute distance measurements at long range,* Nature Photonics **3**, 351 (2009).

[8] J. Ye, *Absolute measurement of a long, arbitrary distance to less than an optical fringe,* Opt. Letters **29**, 1153 (2004).

[9] S. A. van den Berg, S. T. Persijn, G. J. P. Kok, M. G. Zeitouny, and N. Bhattacharya, *Many-wavelength interferometry with thousands of lasers for absolute distance measurement,* Physical Review Letters **108** (2012), 10.1103/physrevlett.108.183901.

[10] Y. C. Eldar and G. Kutyniok, *Compressed sensing: theory and applications* (Cambridge university press, 2012).

[11] C. Lei, Y. Wu, A. C. Sankaranarayanan, S.-M. Chang, B. Guo, N. Sasaki, H. Kobayashi, C.-W. Sun, Y. Ozeki, and K. Goda, *Ghz optical time-stretch microscopy by compressive sensing,* IEEE Photonics Journal **9**, 1 (2017).

[12] D. J. Holland, M. J. Bostock, L. F. Gladden, and D. Nietlispach, *Fast multidimensional nmr spectroscopy using compressed sensing,* Angewandte Chemie **123**, 6678 (2011).

[13] J. C. Vaughan, T. Hornung, T. Feurer, and K. A. Nelson, *Diffraction-based femtosecond pulse shaping with a two-dimensional spatial light modulator,* Optics letters **30**, 323 (2005).

[14] Q. Guo, H. Chen, Z. Weng, M. Chen, S. Yang, and S. Xie, *Compressive sensing based high-speed time-stretch optical microscopy for two-dimensional image acquisition,* Optics Express **23**, 29639 (2015).

ACKNOWLEDGEMENTS

Finally, my thesis comes to this part. It's also the end of the PhD's study. The work presented in the thesis would not be completed without the help and support from you in the past four years.

First of all, I would like to express my sincere gratitude to my promotor, Dr. Nandini Bhattacharya, and co-promoter, Dr. Elizabeth Carroll. Nandini, thank you for your help and advises in research and life. I still remember the first time you helped me to build the distance measurement setup. I learned a lot of alignment skills from your help. When I spoke some stupid ideas to you, you were always patient and friendly. For my first paper, you revised the paper very carefully and corrected the mistakes. The comments from you helped the paper smoothly published. In 2020, the corona virus made the study and life very difficult. Even though we could not have a meeting face to face, you often contacted to me with Whats App. Your encouragement helped me go through the most difficult isolation time and helped me complete the thesis smoothly. Elizabeth, thank you for your help to my graduation and defence. After I moved to medical imaging group, you are very friendly to be my co-promotor, which makes my PhD studies go on smoothly. Without your help my PhD study would be very difficult.

Many members from Optical Research Group offered me a lot of help. Prof. Dr. H. Paul Urbach help me apply for the CSC scholarship. After I came to the Netherlands, Paul arranged meetings every two weeks, which help me start my PhD research. Your critical inputs and mathematical derivation were very valuable for my work. Roland, this thesis can not be completed with your help of the experiment. I deeply admire your profession and erudition. Your engineering knowledge has benefited me a lot. Thim, I still remember the first laser safty course provided by you, which made me know the importance and dangerous of the laser. Silvania and Florian, thank you for giving me the chance to be the teaching assistant of Optics and Microscopy. I really learned a lot from this valuable experience. Aurele, your cooling system for the chip laser measurement help me complete the experiment successfully. Thank you Yvonne for your support and assistance. You were always kindly and helpful for me even though I already left the group. I also would like to express my thank to all others member: Andreas, Fellipe, Iman, Jin, Lauryna, Lei, Matthias, Macro, Min, Paolo, Po-Sheng, Xukang, Priya, Ying, Zheng (Xi), Zheng (Zhu). It is my honor to be a member of the group for two years.

I am grateful to the staff members from Medical Imaging Group who have provided me invaluable help. Annelies and Angela were always kindly and efficient in helping me with all the issues. Henry, you always help me with the devices of the experiment. Nicolette, your management of the group is very successful. I want to thank my colleagues, Fabian, Moein and Ulas. It is very happy to work with you all.

Special thanks go to collaborators, Zhong wen and Guang. Zhong wen and his wife not only help me in the research, but also in the life. We often went to the open market together and had very good weekends. Time flights. I wish we can meet together in

China again. Guang, you are a very good researcher. I learned a lot from you. I would like to thank Dr. Prince Anandarajah and Dr. Aleksandra Kaszubowska-Anandarajah from University of Dublin Trinity College. Your dual comb system is very powerful and easy to use. You really did a good job. I am very happy to work with you. Steven, the research from VSL, you are always kindly and helpful. Every time we want to borrow the HeNe laser, you won't refuse to provide help. I am grateful to Sylwester and Erwin from TUE. The intergrated laser provided really open a new door for distance metrology technique.

I also want to express my gratitude to all my Chinese friends in The Netherlands. Yifeng, you are very smart and can provide opinions in different ways. Zhe, thank you for your help and advises. Shan, who also comes from Northeast of China, thank you for your kindness and help. You are a true Northeast girl. Boling, it is a pity I did not complete the experiment with your sensor. But I think we will have further cooperation after I come back to China. I also thank to Tiexing, Wenxiu, Dong, Qingru. We really had happy hour during the lunch time.

Last but not least, I sincerely thank my parents for their encouragement, support, and love. My dear Dad, you always encourage me to go outside and have a look at the world. When I am in trouble, you will always give me strongest support whenever you are. For now, I am strong enough to face the life and live independently. I will always miss you. Mom, thank you for bringing me to life, teaching me and helping me to be strong. Trust me that the life will be better and better. I will always love you.

Kefei Hei

APPENDIX A: EDLÉN EQUATION FOR CALCULATING THE INDEX OF REFRACTION

Calculating the refractive index is a key step of distance metrology in air. The appendix describes how the refractive is calculated by Edlén Equation, which using wavelength of light and atmospheric parameters (temperature, pressure and humidity of the air). These required steps for calculatin is obtained from NIST website (emtoolbox.nist.gov).
(a) Preliminaries:

- Convert all temperatures to Celsius.
- Convert all pressures to Pascal.

(b) Calculate the saturation vapour pressure:

Table 1: Coefficients for calculating saturation vapor pressure

Constant	Uncertainty	Constant	Uncertainty
$K_1 =$	1167.05214528	$K_2 =$	−724213.167032
$K_3 =$	−17.0738469401	$K_4 =$	12020.8247025
$K_5 =$	−3232555.03223	$K_6 =$	14.9151086135
$K_7 =$	−4823.26573616	$K_8 =$	405113.405421
$K_9 =$	−0.238555575678	$K_{10} =$	650.175348448

$$T = t + 273.15 \tag{1}$$

$$\Omega = T + \frac{K_9}{T - K_{10}} \tag{2}$$

$$A = \Omega^2 + K_1\Omega + K_2 \tag{3}$$

$$B = K_3\Omega^2 + K_4\Omega + K_5 \tag{4}$$

$$C = K_6\Omega^2 + K_7\Omega + K_8 \tag{5}$$

$$X = -B + \sqrt{B^2 - 4AC} \tag{6}$$

$$p_{sv}(t) = 10^6\left(\frac{2C}{X}\right)^4 \tag{7}$$

Table 2: Coefficients for calculating refractive index

Constant	Uncertainty	Constant	Uncertainty
$A =$	8342.54	$B =$	2406147
$C =$	15998	$D =$	96095.43
$E =$	0.601	$F =$	0.00972
$G =$	0.003661		

(c) Define constants. The coefficients for calculating refractive index is shown in Table 2.

(d) Convert the laser vacuum wavelength λ to micrometers and then find

$$S = \frac{1}{\lambda^2} \tag{8}$$

(e) Calculate intermediate results at air pressure p, water vapor partial pressure p_v, and temperature t:

$$n_s = 1 + 10^{-8}(A + \frac{B}{130 - S} + \frac{C}{38.9 - S}) \tag{9}$$

$$X = \frac{1 + 10^{-8}(E - Ft)p}{1 + Gt} \tag{10}$$

$$n_{tp} = 1 + p(n_s - 1)\frac{X}{D} \tag{11}$$

(f) Calculate the final result for index of refraction n, using our variation of the water vapor term:

$$n = n_{tp} - 10^{-10}\frac{292.75}{t + 273.15}(3.7345 - 0.0401S)p_v \tag{12}$$

CURRICULUM VITÆ

Kefei HEI

10-11-1988 Born in Chanchun, China.

EDUCATION

2007–2011 B.Sc. in Information Engineering
Tianjin University, Tianjin, China

2012–2015 M.Sc. in Information and Communication Engineering
Tianjin University, Tianjin, China

2016–2021 PhD.in Applied Scinece
Delft University of Technology, Delft, The Netherlands

LIST OF PUBLICATIONS

5. **K. Hei**, S.A. Van den Berg, G. Shi, and N. Bhattacharya, *Dispersion correction in high-accuracy longdistance measurements based onmode-resolved frequency comb.* (manuscript in preparation)

4. **K. Hei**, K. Anandarajah, E. Martin, G. Shi, P. Anandarajah, and N. Bhattacharya, *Absolute distance measurement with gain-switched dual optical frequency comb.* Optics Express **29**, 6 (2021)

3. G. Shi, **K. Hei**, W. Wang and N. Bhattacharya, *High precision FMCW laser distance measurement system using a tunable laser with modulation range of 88 GHz*, Measurement Science and Technology **31**, 4 (2020)

2. **K. Hei**, G. Shi, A. Hänsel, Z. Deng, S. Latkowski, S.A. Van den Berg, E. Bente and N. Bhattacharya, *Distance Metrology with Integrated Mode-Locked Ring Lase*, IEEE Photonics Journal **11**, 6 (2019)

1. **K. Hei**, J. Yu, J. Wang, W. Wang, S. Jia, Q. Wu, and J. Xue, *Variable frequency range finding technology based on double polarization modulation method and system implementation*, Acta Physica Sinica **63**, 10 (2014)